

EFFECTS OF DESIGN PARAMETERS ON A SINGLE-LAP, BOLTED JOINT; USING  
INTERNAL AND SURFACE STRAIN MEASUREMENT TECHNIQUES

By

John Woodruff

A THESIS

Submitted to  
Michigan State University  
in partial fulfillment of the requirements  
for the degree of

Master of Science

Mechanical Engineering

2011

## ABSTRACT

### EFFECTS OF DESIGN PARAMETERS ON A SINGLE-LAP, BOLTED JOINT; USING INTERNAL AND SURFACE STRAIN MEASUREMENT TECHNIQUES

By

John Woodruff

Composite materials have emerged as a method of engineering high strength structures to specific tasks at a low weight cost. The strength to weight ratio makes composite materials ideal for replacing metal components in vehicles, but the plates have to be thick enough to withstand impacts during service use. Often, the weakest point of any composite panel is the point at which it is fastened to the vehicle frame. A bolting method is identified as the fastening mechanism of choice and is applied to a single-lap joint geometry for this study. Fastening parameters included bolt-to-hole clearance, and the use of inserts.

A combination of measurements taken using embedded fiber optic strain gages, digital image correlation, and stiffness data was used to determine the optimum design characteristics. It was seen that clearance had a negative effect on the stiffness of the joint, increased clearance from the zero percent clearance had an immediate effect on decreasing the stiffness of the joint. Also, the fiber optic strain gages found that there was a significant strain concentration just inside the interface between the overlap of the bolted composite to aluminum plates. Initial increase in clearance was seen to increase this concentration. Also, in studying the use of inserts it was found that an aluminum insert at the largest diameter tested of 0.75" outer diameter was the best performing geometry. Overall, the design recommendations were that there should be minimal to no clearance, with an aluminum insert with an outer diameter of 0.75".

Copyright

John Woodruff

2011

To my family and friends, for their constant guidance and support

## ACKNOWLEDGEMENTS

Completion of this master's degree would not have been possible without the dedication of my research advisor, Dr. Gaetano Restivo. It has been a long path from the day I entered the Composite Vehicle Research Center (CVRC) and Dr. Restivo's research group. Looking back I can understand the way I have been developed as a professional and engineer. Dr. Restivo's guidance provided direction in research, technical support in the laboratory, and in helping that I successfully disseminated the information developed during research to the organizations that support our work. Of course, there are many other intangible professional traits that I have learned through interaction with Dr. Restivo that have led to my own personal success.

Also, I have to thank the faculty of the M.S. committee, Dr. Somerton and Dr. Liu. Both Professors have provided substantial support during the time I spent as a student and researcher. Dr. Somerton has helped lead me through class work as an undergraduate student, a graduate student, as well as provided significant career guidance. Dr. Liu has taught me engineering principles through the classroom and helped ensure that I was successful in fulfilling the thesis requirement of the M.S. degree.

Further acknowledgement must be provided to the staff and other faculty of the CVRC. Dr. Patterson has provided the necessary oversight to align the research with the goals of the facilities funders. Also, Dr. Hong was generous to provide both the work space, and basic equipment necessary to conduct the experiments described in this thesis. Use of Digital Image Correlation (DIC) equipment was provided by Dr. Conway, and his expertise was crucial in conducting a successful experiment.

Lastly, I would not be able to have had the opportunity to attend graduate school if not for the generous contribution of the Tank Army Research Development and Engineering Center

(TARDEC) for funding the researched I performed at the CVRC. Through the support of TARDEC I have been provided with tremendous opportunity to learn research skills, develop knowledge of engineering through a hands-on approach, and disseminate what I have learned to those both inside and outside of the engineering field.

## TABLE OF CONTENTS

LIST OF TABLES	ix
LIST OF FIGURES	x
Chapter 1	
Introduction	1
1.1 motivation	1
1.2 Objective	2
1.3 background	3
1.3.1 purely numerical analyses	4
1.3.2 purely experimental analyses	7
1.3.3 both numerical and experimental analyses	9
1.3.4 fiber optic strain gage studies	14
1.3.5 literature review conclusions	18
1.4 tables and figures	21
1.5 references	31
Chapter 2	
Effects of clearance on thick, single-lap, bolted joints using through-the-thickness measurement techniques	33
2.1 introduction	33
2.2 composite manufacturing	35
2.3 experimental setup	37
2.4 experimental results	38
2.5 discussion	38
2.6 conclusions	40
2.7 table and figures	41
2.8 references	48
Chapter 3	
Joints with inserts; combined strain analysis	49
3.1 introduction	49
3.2 experimental setup	50
3.3 experimental results	52
3.4 discussion	54
3.5 conclusion	56
3.6 tables and figures	59
3.7 references	66

Chapter 4	
Summary and conclusions	68
4.1 clearance conclusions	68
4.2 insert conclusions	68
4.3 design recommendations	70

## LIST OF TABLES

Table 1-1: Two percent offset bearing strength, as determined from stress-strain diagram	23
Table 2-1: Material properties of the composite specimen	45
Table 2-2: Stiffness characteristics of each test configuration	45
Table 2-3: Material properties of finite element components	46
Table 3-1: Material properties of the composite panel in the 1 and 2 directions	60
Table 3-2: Stiffness of the single-lap, bolted joint	61
Table 3-3: Sensitivity test measurements; RSG to DIC comparison	64

## LIST OF FIGURES

Figure 1-1: Hole diameters listed in box, (a) hole in inboard row, (b) hole in outboard row	21
Figure 1-2: strain in bearing plane; $\mu$ = friction coefficient, $\lambda$ = percent clearance	21
Figure 1-3: (left) Hole without insert, (right) hole with insert	22
Figure 1-4: Stiffness comparison for clearance conditions	22
Figure 1-5: Acoustic emissions hits vs. applied bolt torque: (left) 0.5 inch bolt, (right) 0.25 inch bolt	22
Figure 1-6: Bearing strain value comparison for three insert variations	23
Figure 1-7: (left) Stress in bearing plane – pin connected, (right) Stress in bearing plane – bolt connected	24
Figure 1-8: Load vs. Displacement data for four bolt tightness combinations; two bolts used in configuration	25
Figure 1-9: (a) initial contact area, (b) intermediate, (c) final, (d) experiment	25
Figure 1-10: Tested insert geometries	25
Figure 1-11: Normalized WDS output compared to strain: (a) for RG830 filter (b) Interference filter	26
Figure 1-12: Test specimen geometry variations (above), and listing of actual specimens made (bottom)	27
Figure 1-13: Results of tensile and compressive tests	28
Figure 1-14: Longitudinal strain measurement (top), transverse strain measurement (bottom)	29
Figure 2-1: Dimensions of the FOS gage locations within the composite panel	41
Figure 2-2: Location of the gage and edges of specimen	41
Figure 2-3: Gages are glued in place with epoxy resin	42
Figure 2-4: Vacuum bag setup for hand layup process	42

Figure 2-5: (A) Mechanical mounting device, (B) Specimen loaded into MTS	43
Figure 2-6: (A) 0 percent clearance, (B) 3 percent clearance, (C) 5 percent clearance	44
Figure 2-7: Strain Profile for all clearance levels at 6000N	45
Figure 3-1: Lap joint loaded into the MTS machine	59
Figure 3-2: Insert Dimensions	59
Figure 3-3: Locations of RSG gages for sensitivity tests	59
Figure 3-4: Baseline, 12.7mm (0.5") hole diameter with no insert	60
Figure 3-5: Strain profile of 15.875mm (0.625") insert for all three metals	60
Figure 3-6: Strain profile of 19.05mm (0.75") insert for all three metals	61
Figure 3-7: Surface strains in 1-direction taken down the center	62
Figure 3-8: Surface strains in the 2-direction taken above the hole at 6000N	62
Figure 3-9: (a) 15.875mm (0.625") steel insert, (b) 19.05mm(0.75") aluminum insert	64

## Chapter 1. Introduction

### 1.1 Motivation

Large advancements have occurred in the field of composite materials for use in automotive and aerospace application. Advancements have been generated by demands for “greener”, more fuel efficient vehicles that also maintained or increased overall safety capabilities. In order to maintain the safety aspects of a ground transportation vehicle, thicker panels were developed. Panels were made thicker in order to provide a safe ride in a more hazardous environment. Such an environment would include heavy day to day wear and tear, as well as the prospect of collisions with other objects or vehicles. Other hazards, such as projectiles, have been included in this environment when composite panels were to be used in military vehicles. Failure of the composite panel by impact with these objects has been a real possibility.

The location where the composite panel is fastened to the metallic vehicle frame was of great importance. At this location, stress concentrations developed upon impact with objects in the course of the vehicle’s journey. And stress concentrations may cause the panel to fail. If a composite panel was to be utilized to its full potential, then the load transfer between the composite panel and the aluminum frame of the vehicle would have to be further developed. Bolting was chosen as the means of fastening since it provided the fastest method of securing or removing a panel from a vehicle frame, while still providing a strong connection. The single-lap bolted joint was a standard test setup for composite fastening of this type. The test setup consisted of a single composite plate bolted to an aluminum plate of equal dimensions.

Several parameters surrounding the single-lap, bolted joint have significant impact of the strength and load-distribution properties of the joint. One such parameter is clearance between the bolt and the hole. When a clearance existed and the lap joint was being loaded in tension, the bolt would tilt, which provided a variation in the contact surface area between the bolt and the hole surface. A variation in contact surface area allowed strain concentrations to build around narrow segments of the hole. Strain concentrations lead to failures at high loads. Knowing the full effects of clearance can determine when a panel must be removed from field use. Another parameter was the use of a sleeve, or insert, between the bolt and the hole. An insert can help modify the load distribution properties of the joint to alleviate strain concentrations. Several different materials and sizes were available for the insert and provide different responses to the applied load. Optimization of the two joint parameters, clearance and use of inserts, was vital for determining the strongest available joint configuration.

## 1.2 Objective

The overall goal is to determine the optimal design parameters for fastening composite panels to vehicles for use in ground transportation. In order to make such determinations, a strong understanding of the fastening mechanism, the single-lap, bolted joint, must be obtained. To do this, several measurement techniques are employed to take experimental measurements on the surface of the composite panel, and internally. Traditional surface measurement techniques using resistance strain gages are used as well as in addition to more advanced digital image correlation (DIC) techniques, which are brought on to discover full-field strain maps. Internally, embedded fiber optic strain gages (FOSG) will provide experimental measurements right at the strain concentration locations during loading.

As a second parameter of the study, the ability to take strain readings at finite locations within the composite panel is explored. It was a goal of the study to show the reliability of embedded fiber optic strain gages in various geometries and loading conditions.

Lastly, the effects of the parameters of the joint are understood through experimental analysis. Effects of an incremental increase in clearance will be determined. Also, the uses of various material and size inserts will be shown. In the conclusion of the study will come the final recommendations for the most effective geometry of the joint.

### 1.3 Background

Researchers have used numerous tools to develop knowledge on the single lap joint. These tools are identified as two major categories, one being numerical studies, the other being physical experimentation. Numerical studies are done using mainly commercial code such as Abaqus or ANSYS with LS-DYNA, but there are exceptions. Physical experimentations are also common and are carried out through various methods such as resistance strain gages, acoustic testing, digital speckle photography and many others. Often both numerical and experimental studies are used as a means of further validating results for a given experiment. A summary of research performed on variations of the parameters of the lap joint is given here and separated into three categories, purely numerical studies, purely experimental studies, and studies that contain both numerical and experimental work.

### 1.3.1 Purely Numerical Analyses

Further investigation of the behavior of a single lap bolted joint was conducted by Tserpes *et al.* (2002). In this configuration one plate was a composite material while the other was aluminum. This study looked at the constructiveness of using Hashin's failure criteria as well as a modified version of the same criteria to further develop the accuracy of a 3-D numerical model. This model was created using ANSYS FE code and incorporated eight-noded SOLID46 3D ANSYS elements. Hashin's failure criterion incorporated the shear stress contribution toward failure. It was seen in the results of the properly constructed model that both transverse normal and shear stresses affected the matrix strength. Failure was said to occur when the first significant irregularity or change in the slope of the load-displacement curve took place. It was also noticed that the incorporation of the shear stress causes conservative estimates of when failure occurred. Incorporation of the Hashin failure criteria showed improvement since prior to the involvement of this criteria FE results generally failed quicker than an actual specimen would. The model was eventually validated against reference load-displacement data.

Effects of pitch distance, row spacing, end distance and bolt diameter on multi-fastened composite joints has been studied by Chutima *et al.* (1996) to see the influences of such parameters on the load distribution on a double lap joint. A two-dimensional FE model has been employed to investigate these parameters. Results show that friction between the pin and composite plate will have negligible effect on the load transfer between pins. Also, the outboard pin of the inboard row experienced the highest stresses under a load. Further, when the pitch distance exceeded approximately six times the pin diameter, load transfer between pins is almost unaffected. Varying edge distance between one and three times the pin diameter produced a

more uniform load transfer. As far as bolt diameter was concerned, the lesser diameter holes have a higher ratio of radial stress to net tension stress and this trend is represented in Figure (1). In this figure the vertical axis represents the stress in the bearing plane normalized by the net tensile stress seen in the region between outer hole rows.

Effects of friction, clearance, bolt elasticity, stacking sequence and clamp-up on the contact surfaces around the bolt of a double lap bolted composite joint were studied by Chen *et al.* (1995). These results discovered that the shape of the contact surface and the distribution of contact points varied significantly during the whole contact process. Data showed that clearance decreased the load capacity of the composite laminate by increasing strains in the bearing plane, proving to have a negative effect on the design. This data is represented in Figure (2) for two values of friction coefficients and is compared against reference experimental data.

Lastly, it was seen that “proper clamping torque will smoothen the failure of the structure”. This stemmed from the washer causing lower tensile inter-laminar normal stress, or higher compressive inter-laminar normal stress around the boundary of the hole. Verification of this study was obtained through comparison with reference experimentation data.

A study involving metallic inserts was performed by Kradinov *et al.* (2005). This study was performed to determine the results of varying the thickness and lay-up of the laminates, while using metallic inserts, on the overall strength of the joint. To test the thickness variable a double lap joint of two composite laminates sandwiching an aluminum plate was created. The aluminum plate was of a uniform thickness of 0.31”, while the laminate plates vary in cross

section (thickness), and lay-up. The lay-up of each section was [(45/0/ -45/0)2/0/90/45/0]s, [(45/0/-45/0)2/0/90/45]s and [(45/0/-45/0)2/0/90]s and corresponds to areas of cross section thickness of 0.1356", 0.1243" and 0.113" respectively. Data has shown that the magnitude of the radial stresses changed as the thickness of the laminate decreased. However, stress concentration remains similar both in magnitude and behavior no matter the change in laminate thickness. Also, stress distribution on the bolt remained unchanged throughout the varying laminate thicknesses. Single lap joints were tested in this study as well as the double lap. In the case of the single lap joint, the joint was comprised of one laminate plate bolted to an aluminum plate, both with uniform thicknesses of 0.117" and 0.31" respectively. The laminate lay-up was [(45/0/-45/0)2/0/90]s for the composite plate. Three bolts were used to combine the two plates. It is seen in Figure (3) that inserts greatly reduced the magnitude of the stress and altered the behavior of the stress, which is critical to predicting failure.

A study on the effects of clearance in a single-lap, bolted joint were conducted using MSC.marc code by McCarthy *et al* (2003). In the study, a laminate of 5.2mm thickness was bolted to an aluminum plate using a 8mm bolt. Four clearance conditions, values of 0, 1, 2 and 3 percent, were implemented to determine the effects on the stiffness of the joint. The results clearly showed a reduction in stiffness with an increase in clearance. Contact between the bolt and the hole was reduced significantly from the increase in clearance, resulting in the decrease in the load bearing area, and hence stiffness as shown by Figure (4). Good agreement was seen between the finite element analysis and experimental results.

### 1.3.2 Purely Experimental Analyses

Kostreva (2002) conducted acoustic emission non-destructive testing experiments to determine the preload torque limit of bolted single lap composite joints. Each lap in the joint consisted of the same IM7/8552 prepreg material with fiber configurations of  $(n(0, \pm 45, 90))_s$ , where  $n = 3, 4, 5$ . The plates had a smooth finish on both sides and a thickness of 0.132", 0.176", and 0.220". In addition to this, three different bolts sizes, 0.125", 0.250" and 0.500", were initially considered for use, but only the two largest bolts actually performed tests for each laminate thickness. With the use of NAS1587-8 washers and self locking thread nuts it was seen that the bolt threads would shear before the laminate was damaged. Evidence of this is shown in Figure (5), which reflects that bolt failure occurs at approx the 22 ft-lbs range and from inspection of the laminate afterward producing no signs of damage. Differences between the acoustic emissions hits between the graphs are from there being hits registered from the turning of the washer, while applying the torque, for the 0.5 inch bolt, which was eliminated in the 0.25 inch bolt test by applying a calcium grease. These tests indicated that when determining torque preload, there was little to be concerned about in the area of damage to the laminate.

Bolt-hole clearance effects on joint strength are studied by M.A. McCarthy and V.P. Lawlor *et al* (2002). A single lap joint configuration consisting of an aluminum plate and a composite plate meeting ASTM standard D5961/D5961 M-96 with a single, titanium, 8mm bolt was tested and measurements in the bearing plane were taken using extensometers. Also, torque levels of 0.5 Nm, representing a finger-tight configuration, and a torque level of 16 Nm were used on a specimen with a protruding head bolt and a quasi-isotropic layup in the experiment. Another specimen was used with a protruding head bolt, finger-tight configuration and a zero-

dominated layup. Four different clearance values were used in the experiment, those being neat-fit,  $80\mu\text{m}$ ,  $160\mu\text{m}$ ,  $240\mu\text{m}$ , representing clearances of zero percent, one percent, two percent and three percent. It was noted from previous studies that the allowable percentage of clearance decreased with an increased hole diameter. Results from this experiment showed that ultimate displacement was larger for larger clearances. Clearance does result in a change in joint stiffness, with the larger clearance resulting in the lower stiffness. In terms of two percent offset bearing strength, only finger-tight joints with protruding head bolts show a significant effect. An increase in clearance at first provides for an increase in strength, and then a decrease in strength for the larger clearance values, this is seen in Table (1)

Also, there was a trend in the ultimate strength that presented  $80\mu$  as the optimum clearance. For the fully pre-torqued, quasi-isotropic configuration no clear trend was developed.

Herrera-Franco et al (1992) examined the possibility of using a plastic inserts versus aluminum inserts in double lap composite joints. The idea was to determine if using a plastic insert that had material properties weaker than that of the composite plate could then help to plastically deform the insert to fill any void created between the plate and pin during loading. This would in theory increase the contact surface area and lessen strain concentrations. High sensitivity Moiré interferometry was used to measure surface strains in the plates. Results between the plastic insert and the aluminum insert were very different. Both inserts lessened stress concentrations in the bearing plane and in the ligament areas, the plastic insert lessened bearing stress by 50 percent in the area approximately two radii from the hole and the shearing stress by 50 percent in the same area, while the aluminum lessened the bearing stress by

approximately 75 percent in the same region and the shearing stress by about 90 percent in that region. It is interesting that a slight increase in tensile stress is seen in the ligament region for the plastic insert while this stress decreased by about 90 percent for the aluminum insert. This is explained graphically in Figure (6)

### 1.3.3 Both Numerical and Experimental Analyses

In order to use FEA in three dimensions as an effective modeling tool it must be shown to correlate well with experimentation. Three-dimensional FEA can accurately model effects in the third dimension on the lap joint, such as bolt tightness, making it a powerful tool. McCarthy *et al.* (2005) have produced a model which strongly correlated analysis results with what can be expected in physical experiments. Their model was a single lap single bolt configuration with a composite surface mounted upon an aluminum surface and created using the MSC.Marc code. By defining contact bodies as sub-parts of joint components, then using a contact table to define which bodies would come into contact with each other, further computational efficiency was achieved. It should be noted that the more contact surfaces available the higher the computational time. Further, this particular model noticed significant secondary bending which created a saddling effect. Their model tried to minimize overhanging nodes and refined a non-over-lap region. For an even more accuracy, use of assumed strain formulation with first order elements was implemented. There was a routine that allowed separate tensile and compressive properties to be implemented. It was noted in the research that while computational time is decreased by modeling the washers as part of the bolt, it did not accurately model the physical characteristics of the system. Another point was made to use the analytical rather than discrete contact. This is so the outward normal from an element which identifies the stresses on the

element would be continuous in nature between elements rather than piecewise. The piecewise approach did not allow for proper movement of elements about each other and so they get stuck so to speak, which provided an inaccurate model. Good agreement was found between the numerical model created and with the experimentation done using 3mm length strain gages, although some improvements were made.

McCarthy *et al* (2005) examined two methods used to model friction using finite element software and compared the results with experimental data to further understand how to improve finite element modeling capabilities. The code used for numerical modeling was MSC.Marc and the physical experiment was performed on a specimen chosen to comply with ASTM standards and made of a single lap joint of two composite plates with layers made with HTA / 6376 high-strength carbon fiber-epoxy material. The specimen was loaded into a Zwick mechanical testing machine for analysis. The methods of modeling friction in question are a “continuous” friction model and the other is known as the stick-slip friction procedure. These models are used to represent the contact motion and to deal with discontinuities that inherently exist in a function representing such a motion. These discontinuities can cause convergence problems and had to be examined to determine which was more accurate. The continuous model, which uses a continuous function to represent the motion itself, did not match well against experimental results. However, the stick-slip model provided numerical results that closely matched experimental results.

Iancu *et al*, (2005) investigated the stress and strain of the bearing plane of a thick, single lap joint with an aluminum plate and a composite plate bolted together. Measurements were

taken by embedded-polariscope photoelasticity and embedded resistance strain gages. Loading was performed with a dead-weight level system. These results were compared to a FE model created in Abaqus using C3D8I eight-node, solid elements. There was reasonable agreement between experimental and numerical experimentation and it is seen in Figure (8) that the higher the torque applied to the bolt the lower the maximum stress in the plate. However, if a certain value of torque is exceeded, joint failure will occur.

Ekh *et al* (2004) tested for secondary bending in a single lap, multi-bolt joint comprised of a composite plate manufactured from A54/8552, which is a fiber reinforced plastic, and an aluminum plate from AA7475-T76 bolted together using titanium bolts. This study showed that as load increased the bending near the edges of the plate increased, although secondary bending did decrease. Also, bending is seen to be more severe for the composite plate in the region where it does not overlap with the aluminum plate. Results from FE analysis using Abaqus matched well with experimental results found from digital speckle photography (DSP).

John D. Pratt *et al.* (2002) conducted a study to decide what influence the head angle and head size of a countersink bolt would have on single lap single bolt joints for panels constructed of three different materials. These materials were, 2024-T3 clad aluminum alloy, 7075-T6 clad aluminum alloy and annealed Ti-6Al-4V titanium alloy. It was thought that by varying bolt head geometry the joint elongation would vary. Tests were conducted using bolts with geometries that varied five different head angles and five head heights. Results showed that bolt head height had a greater effect on joint elongation than head angle. Also, it was seen that for thinner panels, 80 degree head angle was the optimum design, while for thicker panels the 120 degree head

angle was best. Overall, thinner heads produced the best results due to maintaining the straight hole bearing area. Parameter effects were determined by measuring the deformation energy necessary for a joint elongation equal to 9 percent of the 4.0 mm fastener shank diameter against the panel thickness for the case of 2024-T3 clad aluminum. Varying head angles in ten degree increments between 80 and 120 degrees were incorporated into the tests.

A study conducted by Nassar *et al.* (2007) found strong correlations between the behavior of a composite material in a single lap double bolted joint to the tightness of the bolts themselves. In conducting the study the joint was modeled numerically using Abaqus, which was a 3-D model comprised of Brick-C3D8R elements. The results from the numerical study were then compared to experimental testing performed on a MTS tensile machine for validation with damage assessment done using an optical microscope. Between the two bolts of the joint, four different combinations of tightness were observed. Those combinations being both tight, both loose, one tight and one loose, and then switching which bolt was tight and which one was loose. It was seen that delamination occurred around the surface of the composite for loose bolts. Loose bolts could also cause inter-laminar delamination. When bolts were held tight, the matrix and fiber cracked when the washers were placed eccentrically around the holes. Tightened bolts created lateral support for the joint which ultimately ended up causing fiber compressive failure in the joint. Most importantly it should be noted that two bolts were necessary in order to cause fiber compressive failure in the composite since the lateral support is necessary. It should be observed that there was strong comparison between the numerical results and the experimental results for load displacement data, which is represented for all four

combinations in Figure (11). This data shows how tight bolts are superior to loose bolts by allowing a higher stress prior to bearing failure.

C.T. McCarthy and M.A. McCarthy used the three dimensional model created as mentioned previously to then study the effects of bolt-hole clearance. The model was a single bolt single lap configuration with a composite surface mounted on an aluminum plate with an 8mm hole. It was found that during the loading process the shape of the contact surface and the distribution of contact points would vary. This phenomenon is displaced in Figure (12).

Less of a contact surface is achieved between the bolt and the hole when a clearance was made larger. Measurements show that across the shear plane the contact area is 105 -110 degrees when the clearance was made significantly large. This is compared to 160 – 170 degrees being seen when there is no clearance. Of course, less contact surface and still applying the same load lead to a larger stress on the contact surface. More specifically, the radial stress was seen to increase with increased clearance, as well as the tangential stress to less of a degree. Also, FEA results show that an accurate modeling of the decrease in stiffness of the joint was achieved. Finite Element results compared well with experimental results obtained by 3mm gage length strain gages.

Experiments have been conducted by Camanho *et al.* (2005) to investigate the ability of a metallic insert, which is bonded to the composite material, to strengthen the single shear lap joint. In order to determine the best geometry of the insert, a numerical study on three insert

geometries was performed. Abaqus was used to create a 3-D model comprised of 20-node laminated brick solid elements and the insert geometries can be seen in Figure (13).

It was determined that insert A had the optimum results. Data concluded that the geometry of insert A promotes load distribution to the surface of the laminate and therefore a higher yield load for the adhesive is predicted. With this known the experimental study to determine the damage initiation could be carried out using insert A. In the experimentation the insert was made of aluminum and was placed through two composite laminate sheets of unidirectional Texpreg HS 160 REM CFRP. Also, the insert was secured to the laminate using an epoxy adhesive (Araldite 420A/B). The two composite plates were then bolted together using 6mm diameter steel bolts. The inserts have shown to increase the strength of the lap joints. In fact, damage occurred at only 5.00 Kn load with no insert, but did not begin to be seen until 10.10 Kn when insert A was present. These results were determined using piezoelectric acoustic emission (AE) transducers mounted on the specimen to determine damage initiation.

Conclusions drawn from this study are that the use of bonded metallic inserts increased the failure load, the efficiency of single-shear lap joints, and the load corresponding to the onset of damage in the composite.

#### 1.3.4 Fiber Optic Strain Gage Studies

A complete system for measuring strain using Bragg grating fiber optics strain gages and a wave demodulation system, used as a strain interrogator, was developed and validated by Melle *et al* (1993). Advantages to using this system are rooted in the ability of it to provide a linear

output behavior. This type of output behavior eliminates measured direction ambiguity and provides system interruption immunity, and such immunity would indicate that there is an environmental insensitivity.

A simple setup was developed for testing this strain interrogation system, known as the wavelength demodulation system (WDS). A 1.0 cm Bragg grating in 3M low-birefringent fiber was mounted on a cantilever beam, with an RSG gage mounted on the opposing side. The same setup was created for a 1.5 cm Bragg grating gage made with a high-birefringent E-type fiber, which would eventually be the only gage used in experimentation. The WDS was used with two different filters being applied to the light reflected back from the gage, one for each separate experimental setup. One of those filters was a high-pass RG830 colored glass filter and the other an interference filter. Each setup then provided a different filtering function associated with each filter that adjusts the intensity of the back reflected light from the gage. Different linear regions exist for each filtering function, which allows for a different measureable wavelength domain for each filter

Due to the gage used in experimentation being made of a hi-birefringence fiber, there is a slow and fast axis for the reflected signal. Results showed a sensitivity of  $0.648 \text{ pm}/\mu\epsilon$  and  $0.644 \text{ pm}/\mu\epsilon$  for the fast and slow axis respectively. The intensity of the filtered back reflected light is compared to a unfiltered reference intensity. This ratio of filtered to unfiltered light intensity determined the output of the WDS. An applied strain should provide a linear output relationship to this light intensity ratio since the filtering function is applied through it's linear

range. Actual output of the WDS under each filtering condition is normalized to the value seen at zero strain and shown in figure (16).

It can be observed from these graphs that a slight non-linearity exists. This phenomenon is due to the fiber having a hi-birefringence. This birefringence causes the WDS to have to average the signals of the fast and slow axis to provide an overall output value. However, this problem can be avoided by using a lo-birefringence fiber, and a truly linear output relationship would be found. . Also, for the RG830 filter a range of 35,600  $\mu\epsilon$  was found, compared to just 4335  $\mu\epsilon$  for the interference filter. These values are determined by the limited linear range of the filtering functions.

In a study conducted by Lopez-Anido *et al* (2003) extrinsic Fabry-Perot interferometric (EFPI) fiber optic strain gages were embedded in composite panels made of 14 layers of E-glass unidirectional fiber. The optimum size fiber optic cable was found to be 80-93 $\mu\text{m}$  polyimide and 80-103 $\mu\text{m}$  acrylate coating for testing conducted under longitudinal and transverse tension. Gages were embedded in plies seven and eight in directions parallel and perpendicular to the fibers by being stitched to each ply. Stitching the gages to the plies was determined to be the most effective method of securing them to the ply to prevent slippage, while still remaining non-evasive in nature. It was found that orientating the gages parallel to the surrounding fibers was the optimum condition since this did not allow for large resin pockets to build around the gage. Leads for these gages were made to protrude out of the side of the specimen, known as the ingress/egress point, and were protected with an additional layer of Teflon sheathing over the existing sensor sheathing. Panels were constructed using a vacuum assisted resin transfer

molding process. Tensile and compressive tests were performed on the specimens of various shape and orientation as listed Figure (17).

Results showed that embedded EFPI sensors oriented both parallel and perpendicular to the fiber reinforcement direction did not cause significant detrimental effects on the tensile and compressive modulus or strength of the E-glass/ vinyl ester composites, which is shown in Figure (18).

Also it should be stated that in the most difficult challenge in conducting this research was the prevention of sensor lead damage upon panel construction. Observations during testing showed that a signal loss could occur if the radius of the bend in the cable was less than 12.7 mm (0.5 inches). Another interesting point is that EFPI sensors behave the same whether embedded in the composite material or mounted on the surface due to their insensitivity to transverse strain. This insensitivity occurs due to the air gap between the partial mirrors in the not having a photoelastic effect.

Mawatari *et al* (2008) set out to create a numerical model based on experimental data that could predict the transverse and axial strains seen in a fiber optic strain gage with two Bragg gratings. It has been seen that when a transverse strain is applied to a polarization maintaining fiber and that strain was not equal in value to the Poisson's ratio multiplied by the axial stress, a birefringent condition was created. This condition allowed for two variations of the reflected wavelength to be sent back, one along the fast axis, the other along the slow axis. This change in wavelength from the original input, unstrained signal, can then be used to measure the

transverse strains. Experiments proved that the longitudinal strain varies linearly with the wavelength, while the transverse strains did not. This is seen below in Figure (19).

Initially a linear model was created, but this was not significant due to large errors. These large errors are derived from the fact that the relationship between the transverse strain seen and the wavelength sent back to the interrogator was non-linear. The non-linear model which accounts for this phenomenon is much more accurate as shown in Figure (20).

### 1.3.5 Literature Review Conclusions

The composite to aluminum lap joint has been studied and developed by many research groups. It was seen in these studies that increasing the contact surface area between the bolt and the hole was of great importance in decreasing stress concentrations and improving the strength of the joint. Several factors affect the ability to maximize this contact surface area, and therefore maximize the strength of the joint itself. Some of these factors include bolt-to-hole clearance, the geometry of the hole itself, and whether or not an insert is present in the hole.

Hole geometry was of interest, although few adjustments have been made to the hole in order to increase joint strength. Hole diameter has been studied as a parameter and it was seen in multi-bolt, multi-row specimens that smaller diameter holes lead to higher stress concentrations in the bearing plane as shown in Figure (1). As a further adjustment to the hole-bolt interface, countersink bolts were tested and were shown not to be effective versus bolts that maintain the straight hole bearing area. This trend was displayed best in Figure (8), where thinner heads could withstand higher deformation energies under the same joint elongation. Beyond this there

was little research dealing with changing hole geometry and further work could be employed to study hole geometry as a parameter more fully.

Clearance between the bolt and the hole was a parameter widely studied with very consistent results. In single lap joints, experiments found that large clearances decreased the contact surface area, which lead to larger stress concentrations. In fact, in the study by C.T. McCarthy and M.A. McCarthy, for a hole of 8mm diameter, the contact surface area was decreased from 160 to 170 degrees around the hole for minimal clearances to about 105-110 degrees for larger clearances. This was further looked at with the double lap joint by Chen *et al* (1995) and like the single lap joint it was found that the shape of the contact surface and the load distribution of contact points varied significantly during the whole contact process. This resulted in higher stress concentrations for larger clearances as represented by the presence of high strain values depicted in Figure (2) above. Clearance was looked at from the perspective of finding proper tolerances and interestingly, results showed that for a finger-tight protruding head bolt, a small clearance can provide an increase in joint strength, followed by a trend of decreasing joint strength for any further increase in clearance. Table (1) illustrated that for an 8mm bolt, clearance values between neat-fit and 160 $\mu$ m show the possibility of the bearing plane to hold higher values of stress than when either no clearance is present or values greater than 160 $\mu$ m are present. This trend of seeing a small increase in strength followed by a decrease leaves open the possibility of finding more exact tolerances. Further research should be focused on a narrow range of clearance values in search of finding proper tolerances. Finding these tolerances can include a focused on different hole sizes or the inclusion of pre-tension effects.

The most significant factor in increasing the joint strength has been the inclusion of an insert into the bolting configuration. Aluminum inserts in single lap joints have nearly doubled the load necessary for initiation of damage to the matrix material. In one study of a single lap joint by Camanho, P.P, Tavares, C.M.L., et al. (2005) it was seen onset of damage to the material increased from 5.0 Kn to 10.1 Kn with the inclusion of the aluminum insert and is further illustrated in Figure (12). The idea of using inserts was extended to the multi-bolt setup for single lap joints, which saw a greatly reduced magnitude of the stress and altered the behavior of the stress in the joint as compared to a joint with no inserts. Actually, the radial stress from the hole decreased from about 320 lb/in to approximately 120 lb/in in this joint configuration and is shown graphically in Figure (3). Further development lead to changes in the insert itself. A study using “soft” inserts was conducted in which the “soft” insert is made of a material that would deform under the load and hopefully fill any void between the bolt and the hole, thus increasing contact surface area. However, results showed that this design did not decrease stress concentrations as much as the aluminum insert had. In fact, the soft insert showed a decrease in bearing stress of 50 percent, while the aluminum insert decreased bearing stress by 75 percent, which can be referenced in Figure (5). Still though, insert design remains a promising area of expansion for the study of increasing joint strength with areas such as insert geometry available for future study.

1.4 Tables and Figures

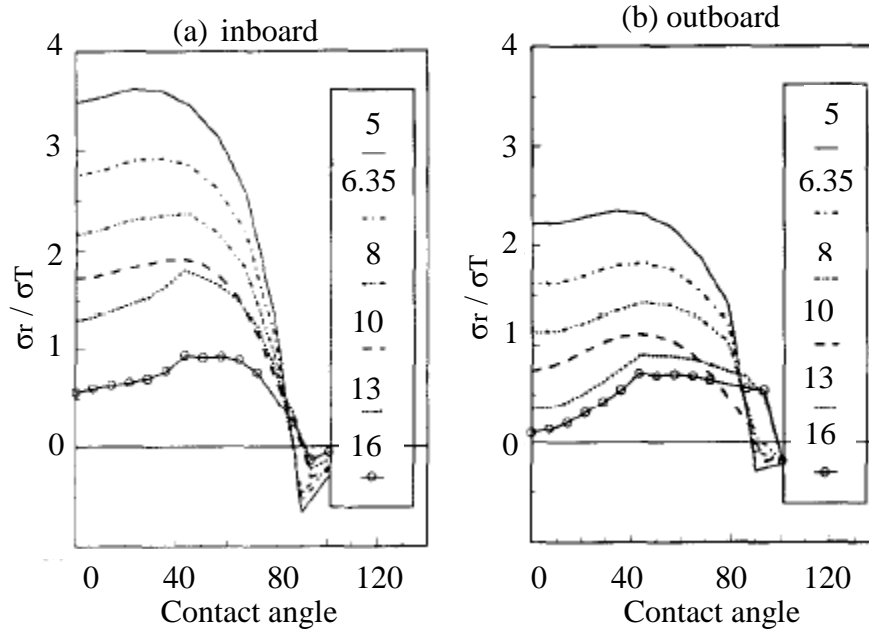


Figure 1-1: Hole diameters listed in box, (a) hole in inboard row, (b) hole in outboard row

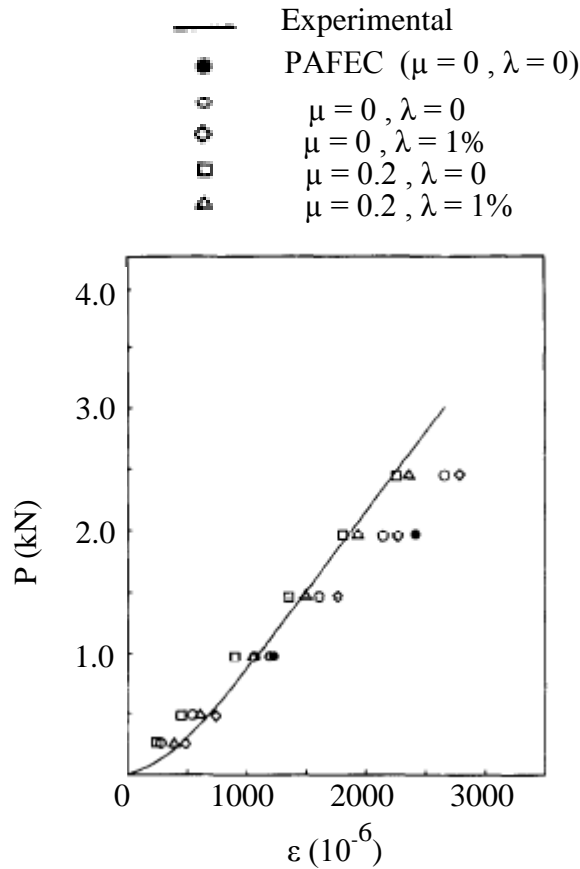


Figure 1-2: strain in bearing plane;  $\mu$  = friction coefficient,  $\lambda$  = percent clearance,

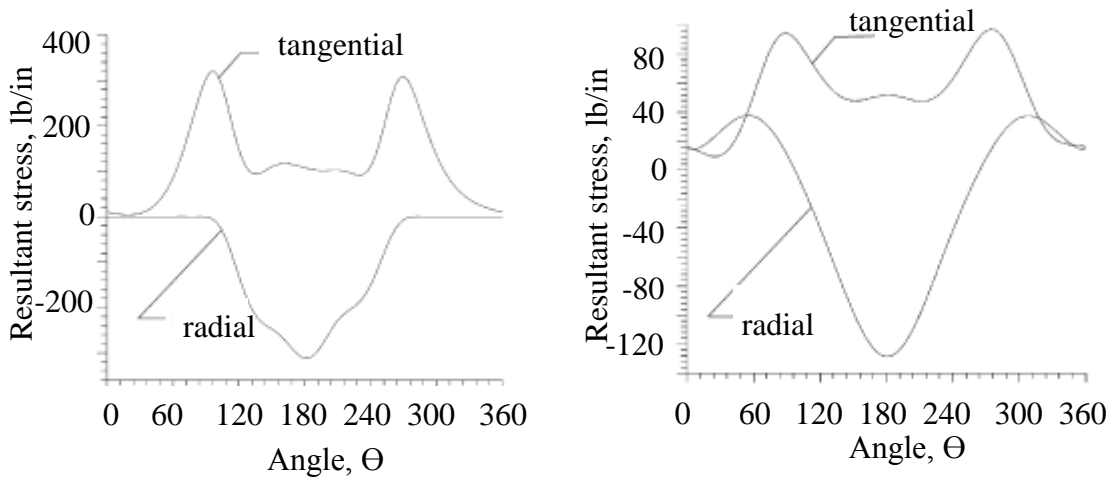


Figure 1-3: (left) Hole without insert, (right) hole with insert

	Neat Fit	80 microns	160 microns	240 microns
Percentage change from C1 (Models)	-	-4.2%	-8.5%	-11.7%
Percentage change from C1 (Experiments)	-	-1.9%	-7.3%	10.4%

Figure 1-4: Stiffness comparison for clearance conditions

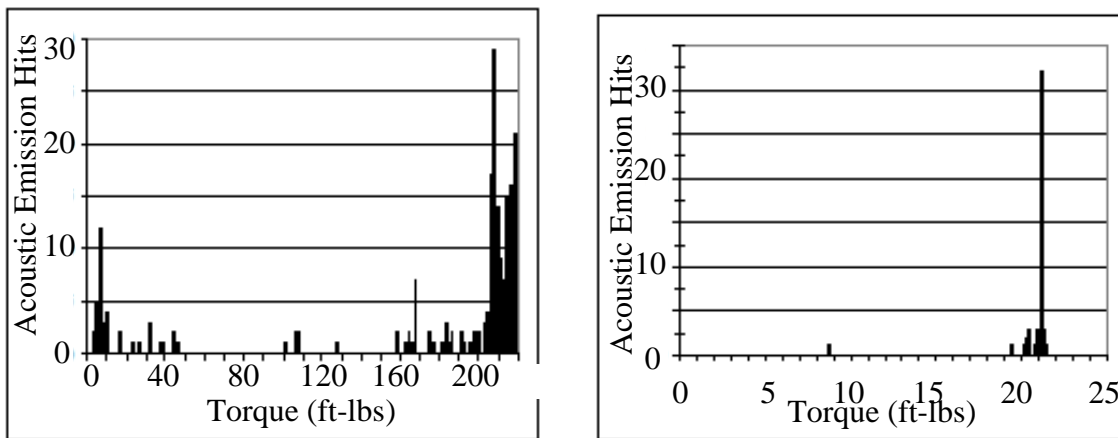


Figure 1-5: Acoustic emissions hits vs. applied bolt torque: (left) 0.5 inch bolt, (right) 0.25 inch bolt

Clearance	neat-fit	80microns	160 microns	240 microns
Average Value (Mpa)	529.8	541.2	517	490
Diff. from Neat-Fit	-	+2.2%	-2.4%	-7.5%

Table 1-1: Two percent offset bearing strength, as determined from stress-strain diagram

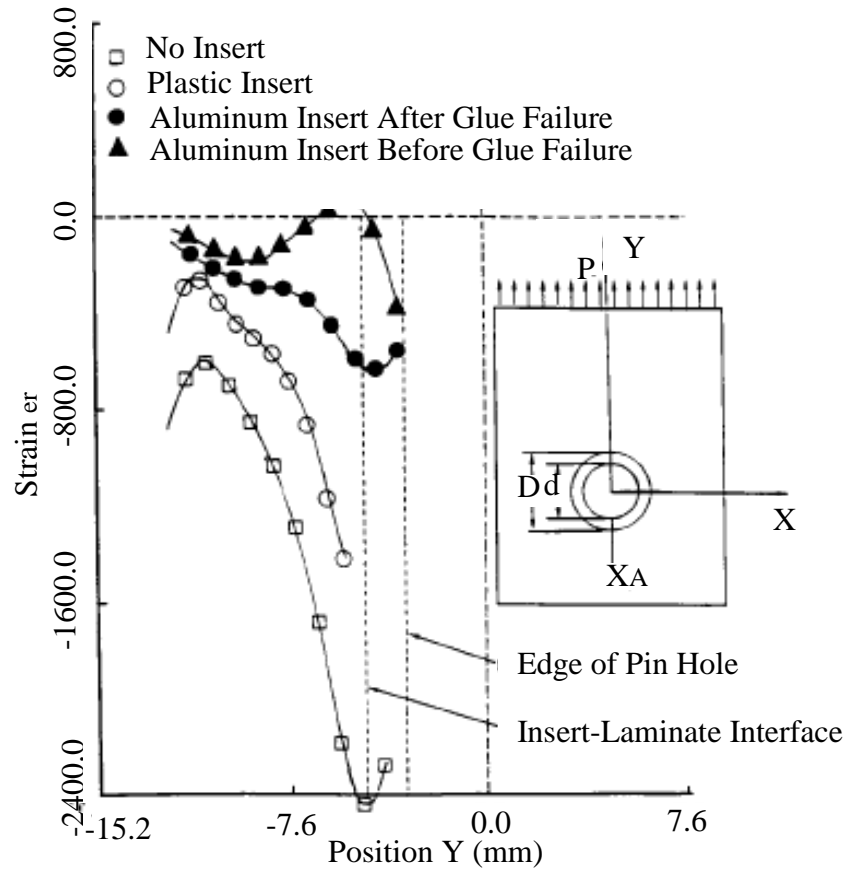


Figure 1-6: Bearing strain value comparison for three insert variations

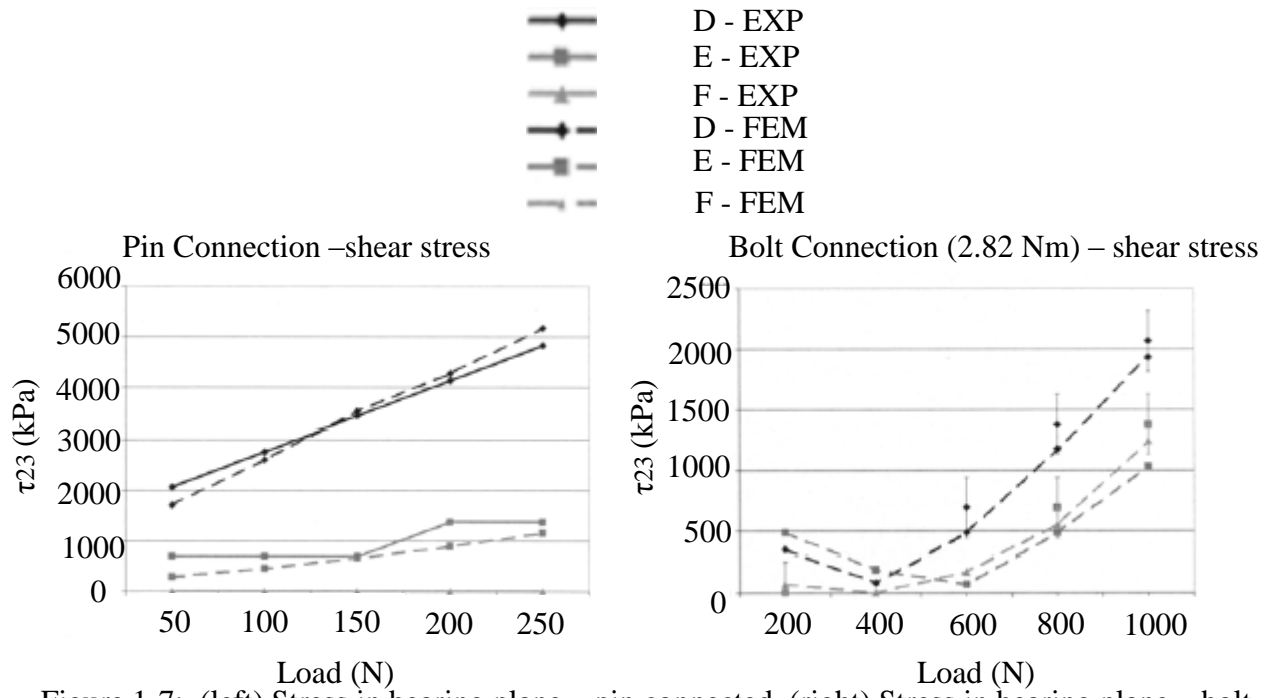
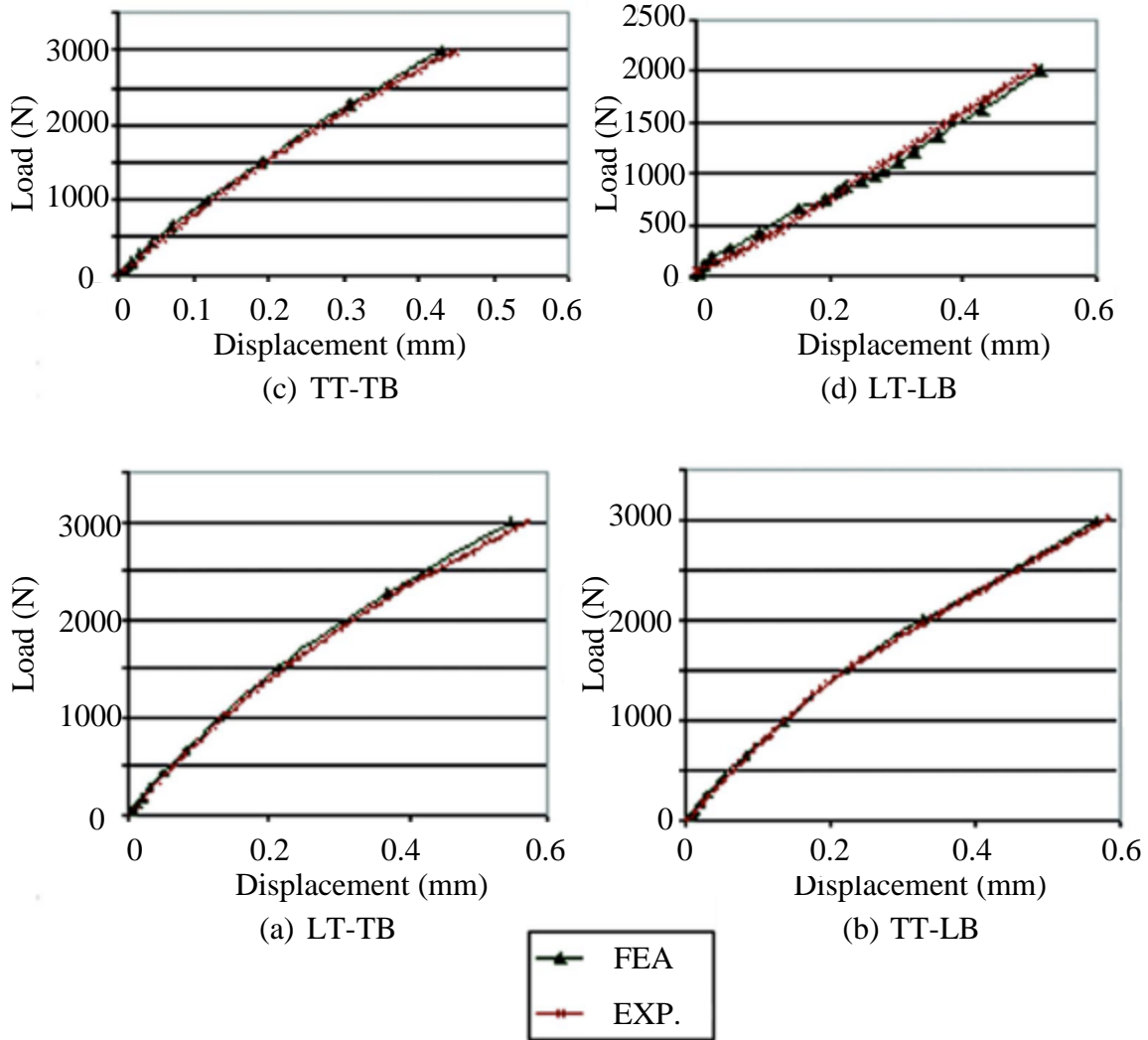


Figure 1-7: (left) Stress in bearing plane – pin connected, (right) Stress in bearing plane – bolt connected



LT-TB = Loose top bolt – tight bottom bolt, TT-TB = Tight top bolt, loose bottom bolt

Figure 1-8: Load vs. Displacement for four bolt tightness combinations; two bolt configuration

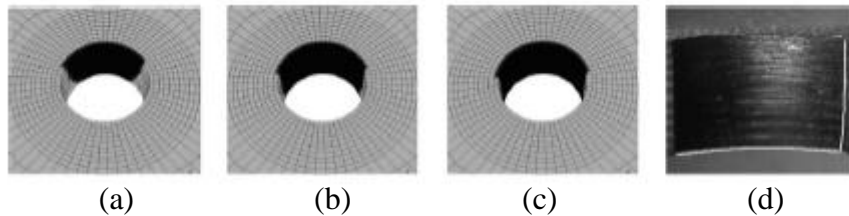


Figure 1-9: (a) initial contact area, (b) intermediate, (c) final, (d) experiment

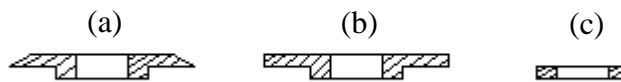


Figure 1-10: Tested insert geometries

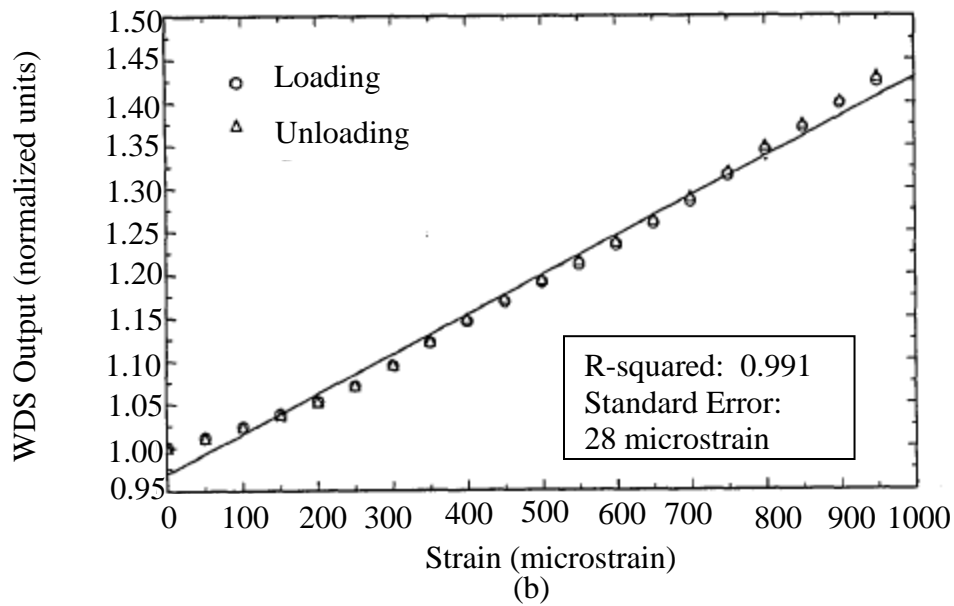
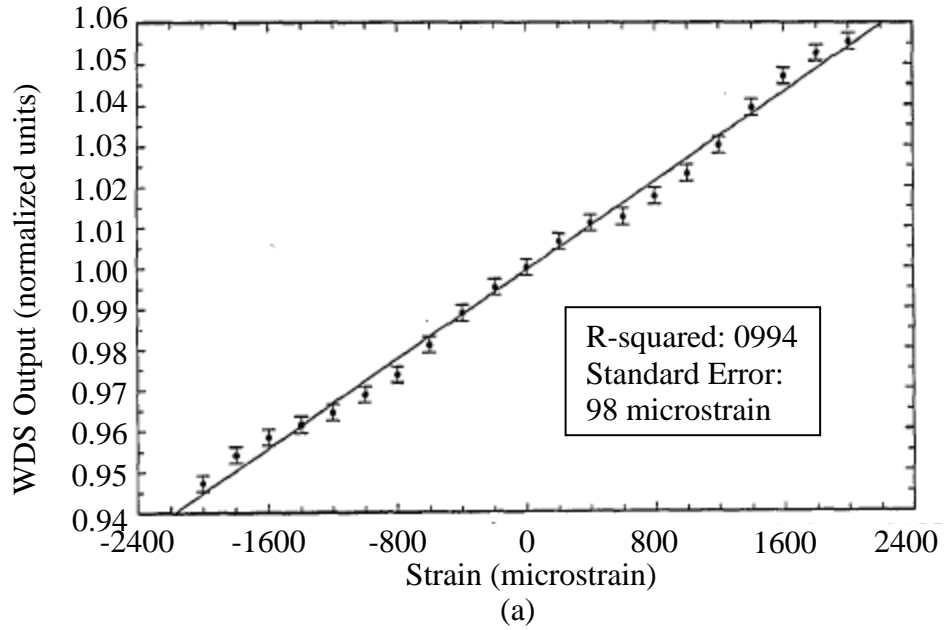


Figure 1-11: Normalized WDS output vs. strain: (a) for RG830 filter (b) Interference filter

**Test Specimen Geometry**

Panel Type	ASTM Test Method	Fiber Reinforcement Direction	Length (mm)	Gage Area Width (mm)	Shape	Tabbing
T0	D3039	0°	250	9	Rectangular	Yes
T90	D3039/D638	90°	250	20	Dog bone	No
C0	D3410	0°	180	12	Rectangular	No
C90	D3410	90°	150	19	Rectangular	No

**Test Specimen: FOS Direction and Lead Routing**

Panels	ASTM Test Method	Panel Thickness (mm)	Number of Test Specimen with Embedded FOS	Number of Controlled Test Specimen	FOS Direction Relative to Fiber Reinforcement	FOS Lead Routing in Grip Area
T0-1 T0-2	D3039	5.37 5.70	5 5	5 5	Parallel	Lateral edge End edge
T90-1 T90-2	D3039/D638	5.42 5.39	5 5	5 5	Perpendicular	Lateral edge
C0-1	D3410	5.56	5	5	Parallel	End edge
C90-1 C90-2	D3410	7.12 4.49	5 5	5 5	Perpendicular	Lateral Edge

Figure 1-12: Test specimen geometry variations (above), and listing of actual specimens made (bottom)

**Effect of Embedded Sensors on Tensile Mechanical Properties**

Mechanical Property	With Embedded Sensors				Control (No Embedded Sensors)			
	Mean (Mpa)	COV (%)	Mean (Mpa)	COV (%)	Mean (Mpa)	COV (%)	Mean (Mpa)	COV (%)
	Panel T0-1		Panel T0-2		Panel T0-1		Panel T0-2	
Fiber Volume Ratio, Vf(%)	54.8		51.7		54.8		51.7	
Longitudinal Modulus, E1t	39,670	3.3	46,347	35.5	39,538	1.8	39,338	4.1
Longitudinal Tensile Strength, F1t	662.1	31.4	486.8	27.6	842.1	3.3	720.6	4.7
	Panel T90-1		Panel T90-2		Panel T90-1		Panel T90-2	
Fiber Volume Ratio, Vf(%)	54.3		54.6		54.3		54.6	
Transverse Modulus, E2t	11960	10.7	12,030	14.2	12,040	9	11,530	3.8
Transverse Tensile Strength, F2t	29.1	16.2	29.32	16.4	31.95	11.5	32.27	4.7

**Effect of Embedded Sensors on Compressive Mechanical Properties**

Mechanical Property	With Embedded Sensors				Control (No Embedded Sensors)			
	Mean (Mpa)	COV (%)	Mean (Mpa)	COV (%)	Mean (Mpa)	COV (%)	Mean (Mpa)	COV (%)
	Panel C0-1				Panel C0-1			
Fiber Volume Ratio, Vf(%)	53				53			
Longitudinal Modulus, E1c	36,190	34.6			39,597	13.1		
Longitudinal Compressive Strength, F1c	426.5	5.7			385.2	25.9		
	Panel C90-1		Panel C90-2		Panel C90-1		Panel C90-2	
Fiber Volume Ratio, Vf(%)	41.4		53.6		41.4		53.6	
Transverse Modulus, E2c	9184	19	11,635	7.9	8,438	11.7	10,249	23.5
Transverse Compressive Strength, F2c	92.35	5.5	100.6	2.8	94.58	4.8	102.8	4.2

Figure 1-13: Results of tensile and compressive tests

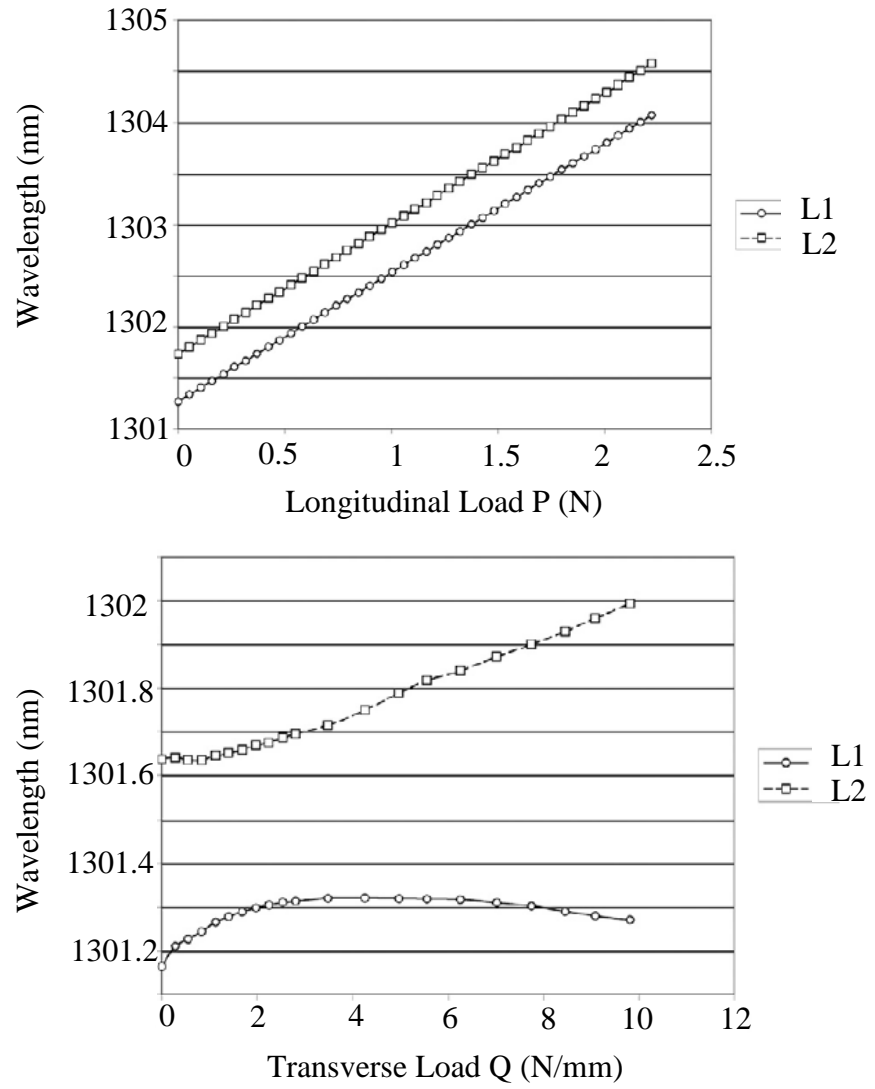


Figure 1-14: Longitudinal strain measurement (top), transverse strain measurement (bottom)

## REFERENCES

## REFERENCES

- [1] Tserpes, K.I., Labeas, G., et al. (2002) "Strength prediction of bolted joints in graphite/epoxy composite laminates." Composites: Part B **33**: 521-529
- [2] Chutima, Surachate, Blackie, Alvin P. (1996). "Effect of pitch distance, row spacing, end distance and bolt diameter on multi-fastened composite joints" Composites Part A **27A**: 105-110
- [3] Chen, Wen-Hwa, Lee, Shyh-Shiaw, et al. (1995) "Three-dimensional contact stress analysis of a composite laminate with bolted joint." Composite Structures **30**: 287-297
- [4] Kradinov, V., Madenci, E., et al. (2005). "Bolted lap joints of laminates with varying thickness and metallic inserts." Composite Structures **68**: 75-85
- [x] McCarthy, M.A., McCarthy, C.T. (2003). "Finite Element Analysis of the Effects of Clearance on Single-Shear, Composite Bolted Joints." Journal of Plastics, Rubber and Composites **32**: 65-70
- [5] Kostreva, K.M. (2002). "Torque Limit for Bolted Joint for Composites Part B Experimentation." NASA Technical Reports
- [6] McCarthy, M.A., Lawlor, V.P., et al. (2002) "Bolt-hole clearance effects and strength criteria in single-bolt, single-lap, composite bolted joints." Composites Science and Technology **62**: 1415-1431.
- [7] Herrera-Franco, Pedro, Cloud, Gary L., (1992). "Strain-Relief inserts for Composite Fasteners – An Experimental Study." Journal of Composite Materials **26**: 751
- [8] McCarthy, M.A., McCarthy, C.T., et al. (2004). "Three-dimensional finite element analysis of single-bolt, single-lap composite bolted joints: part I-model development and validation." Composite Structures **71**: 140-158
- [9] McCarthy, C.T., McCarthy, M.A. et al. (2005). "Experience with Modeling Friction in Composite Bolted Joints" Journal of Composite Materials **39**: 1881-1908.
- [10] Iancu, F. Ding, X. et al (2005) "Three-dimensional investigation of thick single-lap bolted joints." Experimental Mechanics **45**: 351-358
- [11] Ekh, Johan, Schon, Joakim, et al. (2005). "Secondary bending in multi fastener, composite-to-aluminum single shear lap joints" Composites: Part B **36**: 195-208
- [12] Pratt, John D., Pardoen, Gerard. (2002). "Influence of Head Geometry on bolted Joint Behavior" Journal of Aerospace Engineering **15**:4:136-153

- [13] Nassar, Sayed A., Virupaksha, Vinayshankar L., et al. (2007). "Effect of Bolt Tightness on the Behavior of Composite Joints." Journal of Pressure Vessel Technology **129-1**: 43-51
- [14] McCarthy, M.A., McCarthy, C.T. (2004). "Three-dimensional finite element analysis of single-bolt, single-lap composite bolted joints: part II-effects of bolt-hole clearance" Composite Structures **71**: 159-175
- [15] Camanho, P.P, Tavares, C.M.L., et al. (2005). "Increasing the efficiency of composite single-shear lap joints using bonded inserts." Composites: Part B **36**: 372-383.
- [16] Melle, S. M., Liu K., Measures, R.M. (1993). "Practical Fiber-Optic Bragg Grating Strain Gauge System". Applied Optics. **32**: 3601 – 3609
- [17] Lopez-Anido, R., Fifield, S. (2003). "Experimental Methodology for Embedding Fiber Optic Strain Sensors in Fiber Reinforced Composites Fabricated by the VARTM/SCRIMP Process". Structural Health Monitoring 247 – 254.
- [18] Mawatari, T., Nelson, D. (2008). "A multi-parameter Bragg grating fiber optic sensor and triaxial strain measurement" Smart Materials and structures **17**

## Chapter 2. Effects of Clearance on Thick, Single-Lap, Bolted Joints Using Through-the-Thickness Measurement Techniques

### 2.1 Introduction

Clearance between the bolt and the hole of the composite panel has been an important factor in the strength of the joint. When the lap joint was being pulled in tension, the bolt would tilt, which provided a variation in the contact surface area between the bolt and the hole surface through the thickness of the panel. The larger the contact surface area that was maintained during testing, the better the load distribution between the bolt and the hole surface. Initial clearance between the bolt and the hole was seen to have a significant effect of the ability to maintain the maximum surface area contact and the strength of the joint.

In order to properly develop the single-lap, bolted joint, a literature review was conducted to identify the current state of research on the topic. Papers were compiled and reviewed in order to determine what was currently known about clearance in thick composite panels. Studies reviewed included many numerical and experimental techniques.

Initially, the effects of changing the bolt tightness and shape were examined [1]. Results showed that the single-lap, bolted joint maintained a greater stiffness and strength when the bolts used did not have a countersunk head shape. The reason for this was simply that the straight-hole bearing area was maintained for non-countersunk bolts. Also, the tightness of the bolt was examined and experiments clearly showed that a higher torque value produced stiffer joints [2,3].

A study was performed with a thin single-lap joint with an 8 mm diameter hole was tested for small clearance values [4]. It was seen that as clearance increased, the contact surface area decreased from 160 – 170 degrees around the hole for a zero percent clearance condition to 105 – 110 degrees at the largest clearance value of three percent. The same author performed another study which had shown the effects of clearance on stiffness and bearing strength was affected [5]. In this study, increased clearance showed a decrease in joint stiffness. However ultimate bearing strength was not affected by clearance. Other numerical studies had found similar results when clearance was tested to determine the effects [6,7]. One such study concluded that clearance decreased the load capacity of the joint and was overall a negative design characteristic. This was a very general statement, but in line with other research groups findings.

Interest in further analyzing clearance effects on the lap joint has led to developments in measuring techniques. Fiber optic strain gages of various types have been considered for use in taking through-the-thickness measurements within the composite panel. These gages have the advantage of being very small in gage length, are immune to electromagnetic interference and they can be embedded non-invasively into a composite panel [8,9]. The material properties in the region of the gage do not change and point measurements of strain are available. Measurements could then be used to experimentally validate finite element models.

One study exists as an attempt at developing an understanding of the strain profile at low loads [10]. In this study, fiber optic strain gages were embedded within a thick 12.7mm (0.5”) composite panel of the single-lap joint at regular intervals through-the-thickness above the hole.

Measurements using a loading frame setup then provided data for low loads of a strain profile through-the-thickness. Results showed good correlation for pin joint setups with FEA models. However, there was discrepancy between the FEA model for the bolted configuration with the experimental data. It should be remembered that the tests in this study were conducted at low loads.

The next logical step in the development of the lap-joint is to then use embedded fiber optic strain gage technology to understand the effects of clearance. Creating a specimen similar to [10] provides a more thorough understanding of the actual strain profile when tested through a higher loading range. Also, changes in the strain profile above the hole when clearance is present are experimentally determined.

## 2.2 Composite Manufacturing

A composite specimen for testing was constructed using a hand layup process with vacuum bagging. The process included attaching the Bragg grating fiber optic strain gages to the plies prior to creating the specimen. Then, once the gages were secured and their location marked, the layup process began. The plies were inserted with the attached gages in the proper order to know their location in the thickness direction of the final specimen.

The specimen tested was constructed from a plain weave S-Glass material and an epoxy resin. The S-Glass was chosen due to having superior tensile strength than the E-glass. The epoxy resin was 635 Epoxy and used a 3:1 ratio of Epoxy to hardener. The epoxy, hardener and fiber are supplied by US Composites.

The actual dimensions of the panel were chosen as ratios of the hole diameter. The hole diameter was known to be 12.7mm (0.5 inches) for this panel. A thickness to hole diameter ratio of 1:1 was used. Also, the ratio of edge distance to hole diameter was 4:1 moving laterally from the hole, and 3:1 from the top of the plate to the center of the hole. The locations of the gages within the composite plate are shown in Figure (1). The two fiber optic strain gages to be used in this experiment are provided by Technica SA and are located at the places designated as 3 and 4 on the above diagram. In order to obtain data for the 1 and 2 locations the specimen was simply reversed. The gages are Bragg grating fiber optic strain gages and have a gage length of 2mm with a maximum strain output of approximately 12,000 microstrain. The 2mm gage length was chosen since it is small, and works accurately for taking strain readings at specified points in the presence of a large strain gradient. Also, a 3mm protective armor cable was used to protect the internal fiber optic cable from shearing off at the ingress/egress point after construction. Further protection was provided at the adapter, where the cable connects to the interrogator. The FC/APC adapter had attached to it a strain distributing support.

The gages were applied to a ply prior to the hand layup process. This was done by first marking the edges of the specimen and the location of the center of the gage with a thin black cotton string as shown in Figure (2). String was used so that during the layup process the plies with gages can be aligned via the string. Lastly, the gage was glued in place using the same epoxy and hardener that will be used during the hand layup process and is shown in Figure (3).

The composite panel was created large enough so that specimens for tensile tests could be cut from the same panel that the test specimen would be made from. Tensile tests were used to determine the material properties of the composite panel for use in a finite element model used for experimental validation. The hand layup process was performed by inserting the plies with the gages at the desired interval. Overall, 60 plies were used including the two with gages attached. Since the gages were inserted at locations 0.1 inches and 0.2 inches in from the front surface, this meant they were located as plies 12 and 24. A vacuum bag system was used to pull extra resin out of the specimen after the layup process was completed. The setup for the panel construction can be viewed in Figure (4).

### 2.3 Experimental Setup

The embedded, lap-joint specimen was tested using a tensile testing machine. Wedge grips were used to hold in place a mounting device created to hold the specimen. A mounting device was used since the lap joint specimen was too thick to fit into the wedge grips of the MTS machine and is shown in Figure (5). Displacement was set to 1.0 mm per minute and the specimen was loaded from 0 – 10,500 N. This loading range was sufficient to develop a linear trend for stiffness data. Fiber optic strain gage data was compiled by Labview software. Testing was performed to determine the optimum bolt to hole clearance condition. For these tests the hole size would remain constant while the bolt would be varied in diameter to reflect clearance values of 0,1,2,3,4 and five percent. As a precaution testing was first performed on gage locations three and four since lower strains were expected at the gages. After these tests were successfully concluded, tests were carried out for gage locations one and two.

## 2.4 Experimental Results

As mentioned, tensile tests were first performed to determine material properties for use in FEA. Young's modulus for the through the thickness direction was specified as that of the matrix material. Table (1) shows the material properties.

Stiffness testing on the embedded, lap-joint specimen provided results that were similar to what was seen in tests on much thinner panels. The stiffest condition was seen when there was no clearance between the bolt and the bolt hole. All clearance results can be seen in Table (2). The zero clearance condition was seen to be the optimal configuration of the joint, with the five percent clearance the poorest performing configuration.

Fiber optic strain gages have provided very interesting data of the strain profile through the thickness of the specimen as shown in Figure (6). Gage two had higher strains than gage one for all tests. Increased clearance from zero to three percent increased the strain seen at all gage by similar proportions to the values at zero percent. However, once clearance was further increased to five percent only the strains at the gages furthest from the interface between the aluminum plate and the composite panel continued to see increased strain. Strain values at 6000N were averaged for the four tests at each clearance level and compared in Figure (7). In this manner, the effects of clearance on strain concentrations can more easily be seen.

## 2.5 Discussion

Experimentation has shown interesting data on the strain profile during loading for the thick, single, lap-bolted joint as well as the optimum clearance condition. A large strain

concentration existed nearer the interface of the composite and aluminum plates, at the gage one and two locations. The strain concentration was seen to initially increase with clearance until five percent clearance was reached. At five percent clearance, a leveling effect had begun in the strain profile. Also, there is much alignment between the stiffness data created in these tests and what has been seen for similar research projects on joints that were constructed of mainly thinner panels. In the embedded specimen, stiffness was seen to be optimized when clearance does not exist at all. There was an 11.04 percent decrease in stiffness from the zero percent to the one percent conditions. Such a large decrease in stiffness has shown the importance of maintaining a tight tolerance on the bolt-hole clearance for use of such a composite plate when used in field applications.

The strain profile through the thickness at the two gage locations was very revealing. Past numerical studies have all shown that the highest strain values are at the interface of the composite plate and the aluminum plate and decrease substantially away from the interface of the two plates. Experimental evidence provided by the embedded Bragg grating fiber optic strain gages has showed that the highest strain values are located a little further in from this interface at the location of gage two. However, gages one and two did both read substantially higher than gages three and four. The difference in what was seen in experimentation and other numerical studies was largely due to a slight translation of the gages during the hand rolling process, and a stiffening effect in the composite panel near the interface of the two plates.

## 2.6 Conclusions

The focal point of this study was to determine the effects of clearance on the strain profile through the thickness of the specimen and the optimal stiffness value for a thick composite panel. The composite specimen contained 60 layers of S-glass in an Epoxy resin resulting in a 12.7mm (0.5 inch) thick composite panel. Point measurements for strain in the bearing plane of the composite specimen were determined experimentally using Bragg grating fiber optic strain gages embedded into the specimen.

Analysis of the data provided conclusions regarding the effects of clearance on strain concentrations and on the stiffness of the joint. The concentration was highest at gage two, which was toward the front of the specimen, but further into the thickness than gage one. Also, strain seen under three percent of clearance was increased from the zero percent clearance conditions at all gages by approximately the same proportion. A further increase in strain to five percent only resulted in an increase in strain at gages three and four, the gages furthest from the interface between the two plates.

Stiffness was seen to follow similar trends to thin composite panels. Any increase in clearance beyond the zero clearance condition lead to a decrease in stiffness. Zero clearance was then the optimum condition at 10.02 KN / mm and five percent was the least stiff at 8.7 KN / mm. Overall, it was seen that increased clearance decreased stiffness, and any initial increase in clearance from zero percent caused a higher concentration of clearance nearest gage one and two.

## 2.7 Tables and Figures

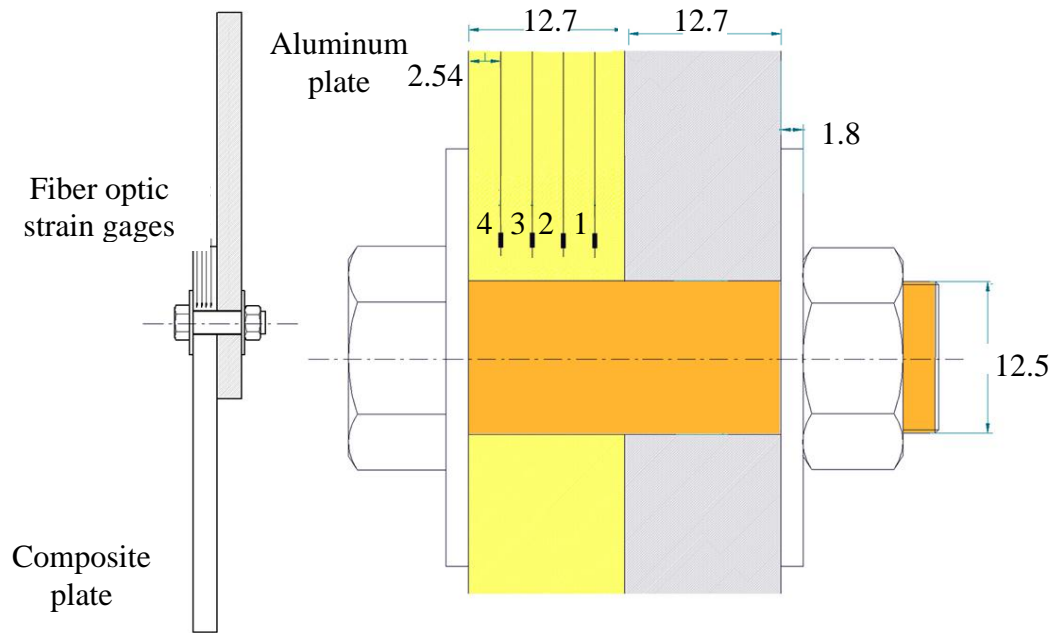


Figure 2-1: Dimensions of the FOS gage locations within the composite panel  
For interpretation of the references to color in this and all other figures, the reader is referred to the electronic version of this thesis

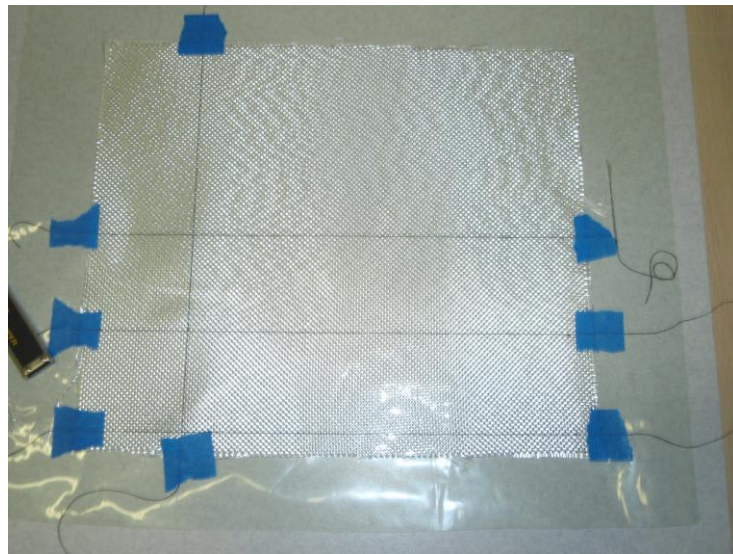


Figure 2-2: Location of the gage and edges of specimen

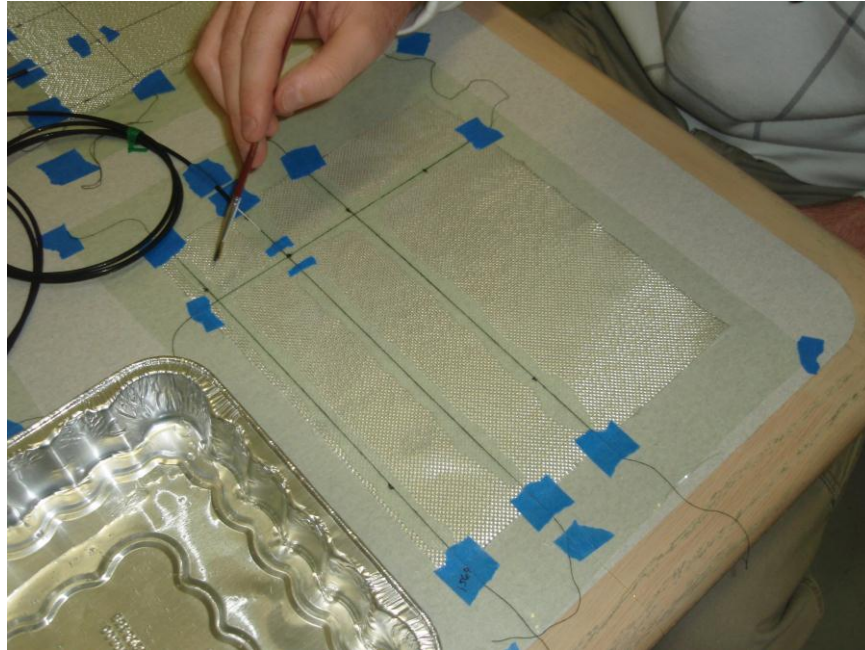


Figure 2-3: Gages are glued in place with epoxy resin

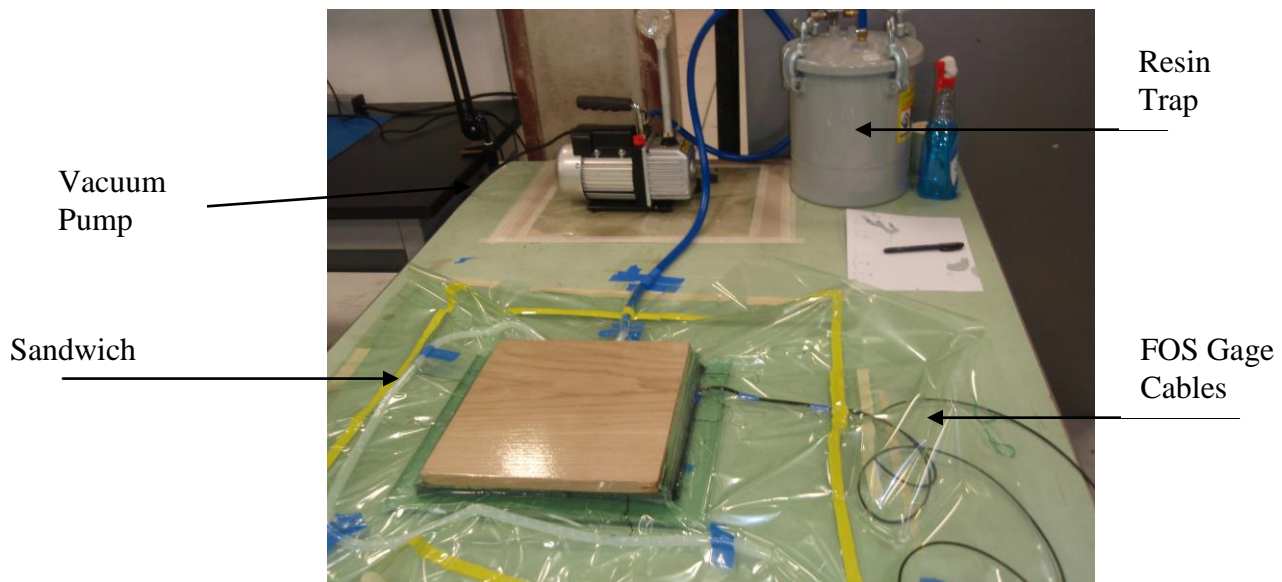


Figure 2-4: Vacuum bag setup for hand layup process

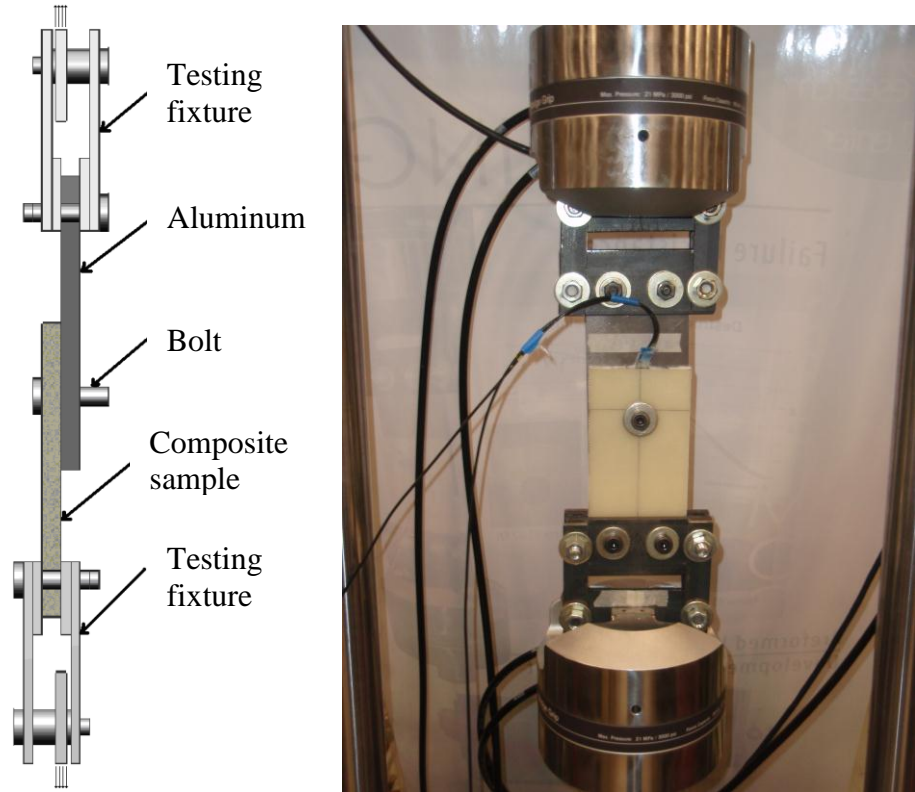
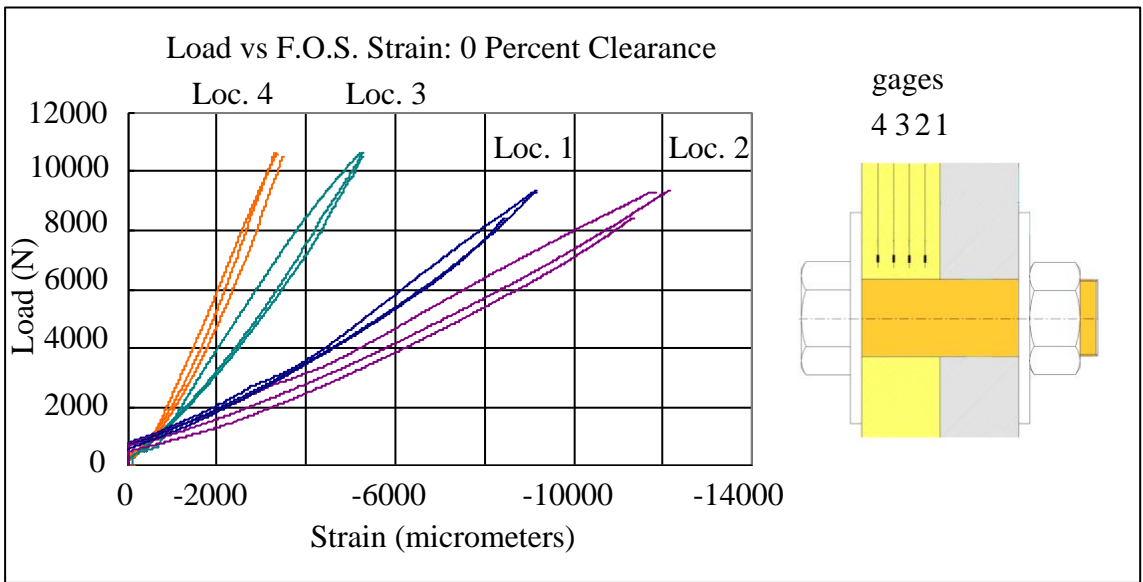
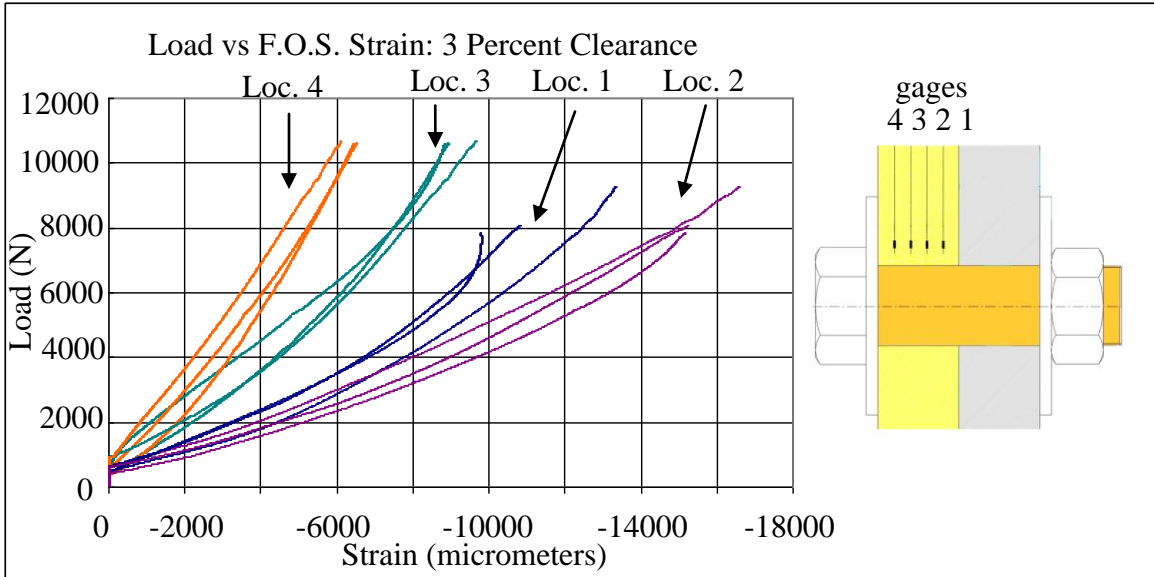


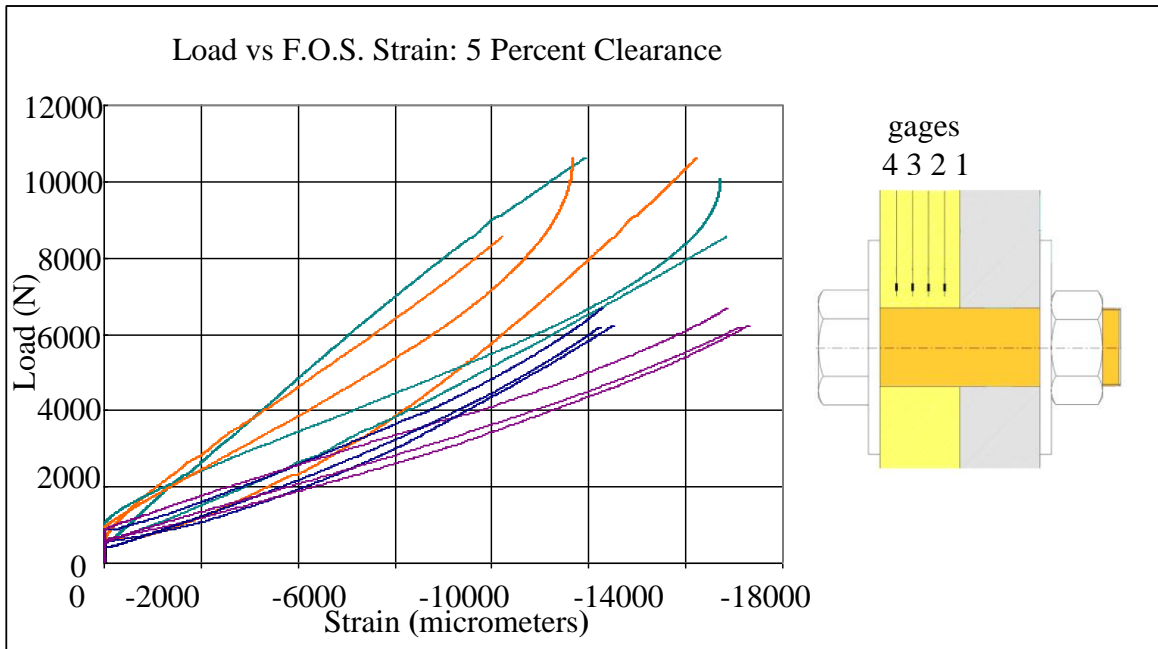
Figure 2-5: (A) Mechanical mounting device, (B) Specimen loaded into MTS



(a)



(b)



(c)

Figure 2-6: (A) 0 percent clearance, (B) 3 percent clearance, (C) 5 percent clearance

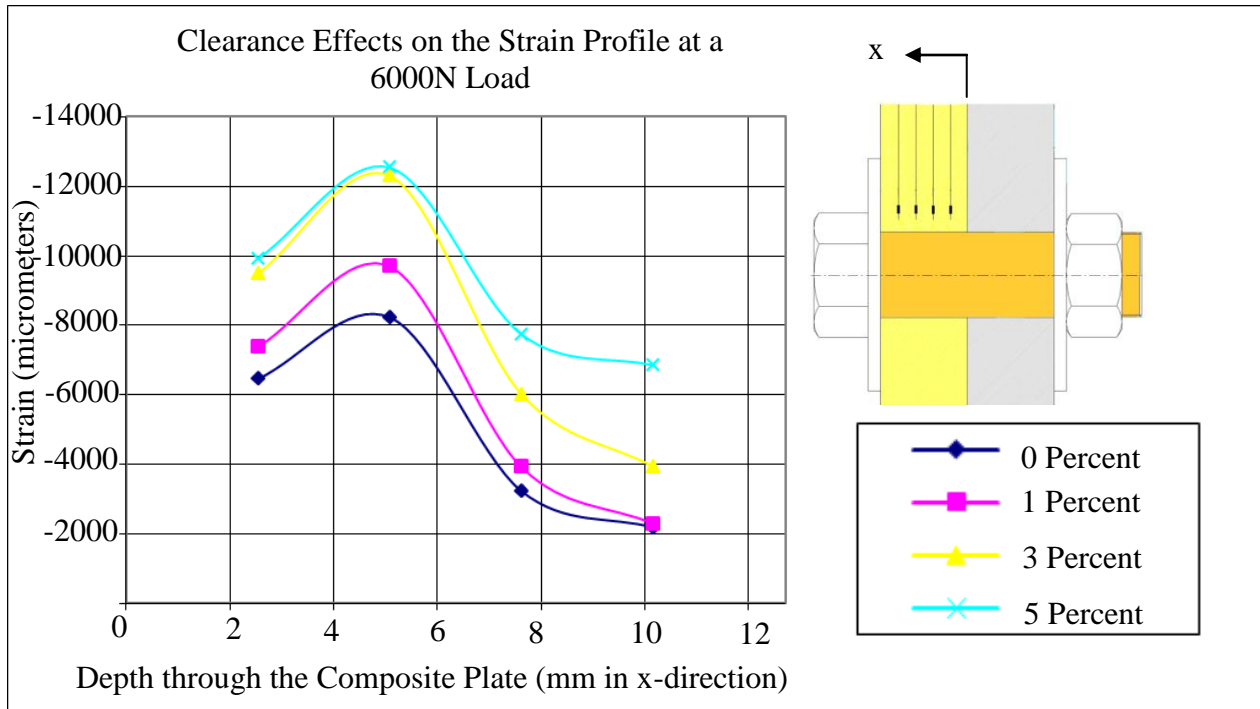


Figure 2-7: Strain Profile for all clearance levels at 6000N

Embedded Specimen	
Ex (GPa)	19.56
v12	0.12

Table 2-1: Material properties of the composite specimen

Embedded Specimen Stiffness Results (N/mm)						
Test #	0%	1%	2%	3%	4%	5%
1	8296	7610	8182	7438	9517	8317
2	10564	7628	7602	8945	8252	9213
3	10858	8438	7859	9133	8977	8273
4	9970	9806	10003	10209	9014	8638
5	10359	10334	10160	9376	9179	8772
6	10387	9947	9973	8963	9621	9040
<b>Average</b>	<b>10072</b>	<b>8961</b>	<b>8963</b>	<b>9011</b>	<b>9093</b>	<b>8709</b>
<b>Δ from 0 (%)</b>	N/A	-11.04	-11.01	-10.54	-9.72	-13.54

Table 2-2: Stiffness characteristics of each test configuration.

<b>Material Properties</b>	<b>E<sub>x</sub> (GPa)</b>	<b>E<sub>y</sub> (GPa)</b>	<b>E<sub>z</sub> (GPa)</b>	<b>V<sub>xy</sub> (GPa)</b>	<b>V<sub>xz</sub>=V<sub>yz</sub> (GPa)</b>	<b>G<sub>xy</sub> (GPa)</b>	<b>G<sub>xz</sub>=G<sub>yz</sub> (GPa)</b>	<b>Density (Kg/m<sup>3</sup>)</b>
Aluminum 7075	72	72	72	0.33	0.33	28	28	2800
Steel Bolt	200	200	200	0.3	0.3	77.2	77.2	7860
Washer	200	200	200	0.3	0.3	77.2	77.2	7860
Composite Plate	19.546	19.546	3.3	0.121	0.11	2.9	1.9	2700

Table 2-3: Material properties of finite element components

## REFERENCES

## REFERENCES

- [1] Pratt, John D., Pardoen, Gerard. (2002). "Influence of Head Geometry on bolted Joint Behavior" Journal of Aerospace Engineering 15:4:136-153
- [2] Iancu, F. Ding, X. et al (2005) "Three-dimensional investigation of thick single-lap bolted joints." Experimental Mechanics 45: 351-358
- [3] Nassar, Sayed A., Virupaksha, Vinayshankar L., et al. (2007). "Effect of Bolt Tightness on the Behavior of Composite Joints." Journal of Pressure Vessel Technology **129-1**: 43-51
- [4] McCarthy, M.A., McCarthy, C.T. (2004). "Three-dimensional finite element analysis of single-bolt, single-lap composite bolted joints: part II-effects of bolt-hole clearance" Composite Structures **71**: 159-175
- [5] McCarthy, M.A., Lawlor, V.P., et al. (2002) "Bolt-hole clearance effects and strength criteria in single-bolt, single-lap, composite bolted joints." Composites Science and Technology 62: 1415-1431.
- [6] Chen, Wen-Hwa, Lee, Shyh-Shiaw, et al. (1995) "Three-dimensional contact stress analysis of a composite laminate with bolted joint." Composite Structures **30**: 287-297
- [7] McCarthy, M.A., McCarthy, C.T. (2003). "Finite Element Analysis of the Effects of Clearance on Single-Shear, Composite Bolted Joints." Journal of Plastics, Rubber and Composites **32**: 65-70
- [8] Baldwin, C., Mendex, Alexis. (2005) "Introduction to Fiber Optic sensing with Emphasis on Bragg Grating Sensor Technologies; short course 102" Course Presented: SEM Annual Conference and Exposition on Experimental and Applied Mechanics
- [9] Lopez-Anido, R., Fifield, S. (2003). "Experimental Methodology for Embedding Fiber Optic Strain Sensors in Fiber Reinforced Composites Fabricated by the VARTM/SCRIMP Process". Structural Health Monitoring: 247 – 254.
- [10] Isaicu, Gabriel (2006). "Three-Dimensional Strain Analysis of Single-Lap Bolted Joints in Thick Composites using Fiber-Optic Strain gages and Finite Element Method" Master's Thesis, Department of Mechanical Engineering, MSU
- [11] Marannano, G., Restivo, G. et al (2010). "GIUNZIONI BULLONATE FRA COMPOSITO E ALLUMINIO: STUDIO DEL GIOCO MEDIANTE FIBRE OTTICHE

## Chapter 3. Joints with Inserts; Combined Strain Analysis

### 3.1 Introduction

Of interest in this study, are the effects of using metallic inserts to improve the strength of the bolted joint. Inserts can improve the contact surface area created between the bolt and the hole, thus improving the strain distribution around the hole, leading to a stronger overall joint. Stiffness will be tested as well as the actual buildup of strain concentrations above the hole by use of fiber optic strain gages (FOSG).

To properly investigate the improvement of the single-lap, bolted joint using inserts, a review of previous work in the area was conducted. The review helps to understand the current state of the technology in order take the most appropriate steps in advancing the state of the technology.

Fastening parameters affecting strain distribution around the bolt hole help to define the proper geometry to explore in the single-lap, bolted joint. Bolt diameter has a great impact on the distribution of stress from the bolt, to the composite plate. Naturally, a thinner bolt is known to provide higher strain concentrations near the contact of the bolt and hole due to the existence of a smaller contact surface area [1]. In the aerospace industry the use of countersink bolts is common practice. The effects of this bolt geometry have been shown to decrease the stiffness of the joint [2]. Tightness of the bolt is a strong factor in distributing loads. Higher torque values provided for stiffer joints [3,4]. Overall, a protruding head bolt, in other words not a countersink bolt, is shown to be most effective in conjunction with thicker bolts in maintaining joint strength.

To provide the strongest panel, the maximum contact surface area between the bolt and the hole must be maintained. A tilting of the bolt occurs during the loading process since the two panels in a single-lap, bolted joint overlap instead of being completely in line with each other. Any clearance between the bolt and the hole will only serve to further decrease the contact surface area and decrease stiffness [5,6,7,8]. Also, the use of metallic inserts has shown the ability to greatly increase the stiffness of the joint [9,10].

Initial studies have been performed to show that fiber optic strain gages can be successfully used to take internal measurements in composite panels. Embedded fiber optic strain gages have shown to be non-invasive to the material properties of the composite [11,12]. The embedding method has been used to take an initial look at the strain profile above the hole in the single-lap, bolted joint configuration [13,14]

### 3.2 Experimental Setup

A second composite panel was constructed in the same manner as in the previous experiment, with a hand layup process with vacuum bag assisted curing. Different in this experiment from the previous, however, is that four gages are embedded, so the panel does not need to be reversed to obtain strain readings at four locations during testing. All four gages were separated by equal distances. The composite panel manufactured and used in the lap joint setup was tested to determine the effects of the use of an insert surrounding the bolted hole. Inserts were cut to two different sizes and constructed of steel, aluminum or brass. Fiber optic strain gages were used to determine the strain profile above the hole during loading. Also, digital

image correlation (DIC) was used to determine surface strains on the free face of the lap joint. Lastly, stiffness of the joint was determined using load and displacement data collected by an MTS machine. The combination of all three measurement sources, FOS gages, DIC surface measurements, and MTS data provided a strong, experimentally determined knowledge of the single-lap, bolted joint mechanics

To apply the tensile load, an MTS 810 was utilized. By themselves, the composite plate and the aluminum plate are too thick to be gripped directly by the MTS machine. The single-lap, bolted joint was then placed into a special loading device that could then be gripped by the MTS. A picture of the mounting device with the lap joint loaded into it is shown in Figure (1). Once loaded into the MTS, a displacement driven loading rate of 1.0 mm per minute was applied. To protect the gages, the loading was kept below 8,000N.

Initially, the hole size was left to 12.7mm (0.5") and no insert was used. A 12.7mm (0.5") diameter steel bolt was used for fastening in all experiments. Both the strain profile above the hole, using the average of the values determined from four tests using the fiber optic strain gages was taken, and then the DIC measurements were taken without an insert present. Next, the hole was widened to 0.625", and an insert of the same outer diameter was placed into the composite and aluminum plates. The insert was one solid piece extending between the two plates and once again, a 12.7mm (0.5") diameter bolt was used. Both FOS and DIC tests were again conducted in the same manner as without the insert. Finally, the hole is once again widened to 0.75" and inserts of the same material, but larger outer diameter are inserted for testing. All insert dimensions are shown in Figure (2).

Once all DIC experiments under all configurations were completed, sensitivity tests were performed to determine the accuracy of the DIC measurements. A steel 0.75” outer diameter insert was used in the experimental configuration. The sensitivity tests were performed by applying two resistance strain gages to the surface of the specimen. These gages were applied 15mm above the hole, and separated 25mm from a line running vertically down the center of the specimen and are shown in Figure (3). Measurements from the two surface gages were compared to strains recorded from the DIC measurements in the y-direction.

### 3.3 Experimental Results

Initially, tensile tests were performed to determine the material properties of the composite panel. The panel was pulled in tension unidirectional by the MTS machine while resistance strain gages mounted onto strips of the composite panel recorded strain values. Tests concluded by determine the material properties shown in Table (1).

Next the composite panel in the single-lap, bolted joint setup was installed into the MTS machine. This panel was tested for the strain profile through the thickness of the panel using the embedded fiber optic strain gages. Five tests were for the baseline, and four tests for all configurations involving inserts were performed and averaged, with the exception of the thinner diameter aluminum insert, which had three tests. Results of the tests for the baseline test, the 15.875mm (0.625”) and the 19.05mm (0.75”) outer diameter inserts are compiled and shown in Figures (4-6).

MTS data provided stiffness data for the single-lap bolted joint. Stiffness data was recorded for the same tests the FOS data was recorded. After averaging, the data was compiled into Table (2).

Surface strain data was collected for strain in the 1 and 2 directions, as well as graphics displaying the full field strain map. The full field strain map of the configurations that have performed the best at distributing the load applied have generated for the sake of being concise.

The strain in the 1-direction is taken across a line spanning the center of the plate from the bottom to the top and is shown in Figure (7). Similarly, strain in the 2-direction is taken across a single line. However, this line spans from the left to the right side of the plate, and just above the washer's top edge. Results of strain the 2-direction are displayed in Figure (8). The full field results shown encompass the entire region surrounding the hole and washer. In Figure (9) the strain map is displayed for strain in the y, or 2-direction. Table (3) shows the sensitivity test data, comparing RSG gages to DIC measurements.

After all analysis was complete, the composite specimen has been analyzed internally, and externally. Internally, fiber optic strain gages revealed the strain profile through the thickness of the specimen. Stiffness results were analyzed using data collected by the MTS machine. Lastly, surface strains were recorded using DIC. All these measurement techniques combined to provide a robust analysis of the single-lap, bolted joint under experimentation.

### 3.4 Discussion

All three measurement sources of measurement helped reveal some interesting mechanics of the single-lap, bolted joint. FOS data provided a strain profile through the thickness of the composite panel in the plane where contact between the bolt and the hole is first made. Also, Stiffness was determined from MTS data, while DIC revealed surface strains. Together, the compiled data converged upon similar trends.

Fiber optic strain gage data have revealed the effects of the inserts on load distribution internal to the panel. When comparing strain values for each insert, it is important to remember that the location of the embedded gages does not change within the panel, the hole is simply widened. What that indicates is that as the hole size increases, the gages become closer to the area of contact between the insert and the composite plate. Despite the closer proximity of the gages to the area of contact and the more intense regions of the strain gradient, the strain value of the best material insert for each size did not produce higher strain values than the baseline. For the 15.875mm insert, the steel, or more rigid insert provided the lowest strain values. With the 19.05mm insert, the softest material, aluminum, provided the lowest strain values. When comparing the baseline to the best insert for each size, the strain values of both inserts saw decreases at all gages. Strain at gages three and four was almost completely eliminated. Since the gages are closer to contact for increasing insert size, and thus hole size, the best load reducing configuration was the aluminum 19.05mm (0.75”) insert. Despite being closer to the contact, the strain profile did not increase in value from the steel 15.875mm (0.625”) insert.

Data from the MTS machine helped describe the overall displacement of the joint during loading. Interestingly enough, there was little difference in stiffness from the baseline, to the smaller inserts. However, when the inserts were increased in diameter, a small, but noticeable decrease in stiffness occurred. This decrease is possibly due to a more significant decrease in the cross sectional area of the tension bearing portion of the composite pane located to the left and to the right of the bolt. Overall, stiffness was not largely affected by the presence of the inserts.

Surface strains for the composite specimen were compiled by a digital image correlation. Data was analyzed graphically for areas of interest, and two-dimensional strains maps were created for the entire exposed surface of the lap joint. The baseline configuration of no insert showed the most intense y direction strains across the specimen. Most significantly, the presence of any insert greatly reduces surface strains over the baseline, and the larger inserts appear to have the most significant effect. Also, it is seen from the same figure that the steel insert with the outer dimension of 15.875mm has the lowest surface strains in the y-direction. The aluminum insert is seen to have the lowest strain for the insert with a 19.05mm outer dimension. Results for the FOS strain gages showed the same results for strains in the y-direction located just inside from the surface represented with this data.

It should be noted however that the sensitivity of the DIC system is a concern. Several factors of the experimental setup affect the sensitivity, those being the grid spacing and facet size for measurements within the software, also, the size of the area of measurement, the out of plane displacement of the specimen during loading, lens imperfections, and the speckle pattern.

Full field strain maps have shown the effects of secondary bending. Below the washer and hole the strain in the 2-direction is compressive. So although the plate is pulled in tension, the effect of bending is the greatest force in the superposition of the two stresses. Also, the bending effect is eliminated just after the center of the hole, which is why the plate then only sees tension in the 2-direction. Overall strain values are much smaller on the surface than in the interior of the specimen. Also, comparison of DIC to RSG data in the sensitivity test showed a good correlation between RSG and DIC data for location 1. However, at Location 2, there was a large discrepancy averaging 190 micro-strain. This might have been due to out of plane displacement of the specimen, or a poor speckle pattern in the region. There was a wide variation in values of the DIC readings at this location, while the RSG were much more consistent.

Considering all the measurements taken, the single-lap, bolted joint has been thoroughly analyzed both internally, and on the surface. Measurements taken from all the utilized sources confirm similar results for the effects of joint strength using inserts of various metals and sizes.

### 3.5 Conclusions

Overall, the different configurations of the single-lap, bolted joint provided for seven different design possibilities. Data from numerous tools converged on the same results providing a validation of each test method. With this in mind, it is clear that the optimum design is the joint that incorporates the aluminum insert at 19.05mm (0.75").

Fiber optic strain gage data has revealed that an increase in the size of the insert provided a decrease in the strain intensity in the bearing plane, above the hole. Interestingly, the stiffer steel insert was the optimal design for the smaller insert size, while the aluminum insert was more ideal for the larger insert size.

Using digital image correlation, the recommendation of using the steel insert at the smaller dimension, and the aluminum at the larger was validated. Both of those inserts produced the smallest amount of strain above the hole for their corresponding insert size. Although, an important fact remains that the strain on the outer surface of the composite panel is dramatically smaller than that seen internally, especially nearest to the interface of the aluminum and composite plates. Sensitivity measurements have shown that DIC data in these tests were not as consistent as the other measurements methods used in this study.

Stiffness, as determined from the MTS data was the most interesting. While there was little change overall in stiffness between any of the tests, it was clear that a minor decrease in stiffness occurs for the larger inserts. Most interesting about this trend is that the larger inserts showed an ability to decrease the strain above the hole the most significantly, as shown with FOS and DIC. A conclusion can then be drawn then that the reason for the decrease in stiffness is most likely due to the decrease in the cross-sectional area of the composite material created from the increased size of the hole to accommodate the insert. In support of this idea, was the fact that the softer insert was most effective for the larger inserts tested. With the increased displacement of a less stiff joint, an insert that could more closely conform to the hole, such as with a softer material like aluminum over steel, would be most effective. In light of all the data

collected, it is clear that the aluminum insert of outer dimension 19.05mm was the most effective insert.

3.6 Tables and Figures



Figure 3-1: Lap joint loaded into the MTS machine.

st	al	br	Thickness	Outer Dia.
			0.125"	0.75"
			0.0625"	0.625"

Figure 3-2: Insert Dimensions

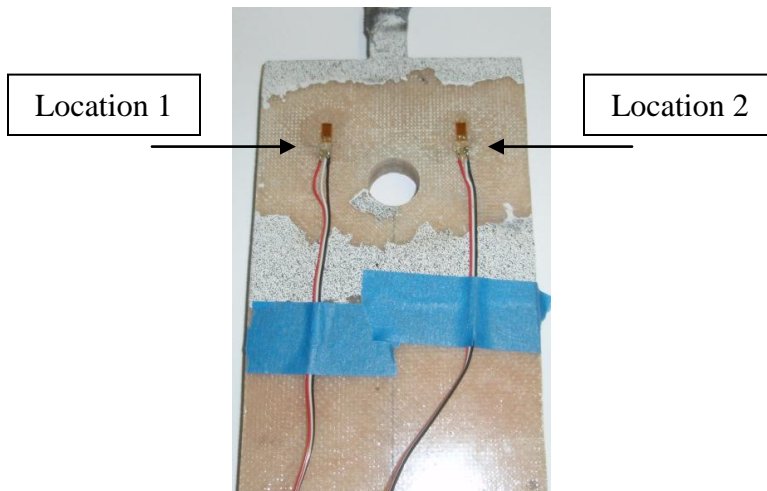


Figure 3-3: Locations of RSG gages for sensitivity tests

E <sub>x</sub>	18.663 Gpa
V <sub>12</sub>	0.113

Table 3-1: Material properties of the composite panel in the 1 and 2 directions

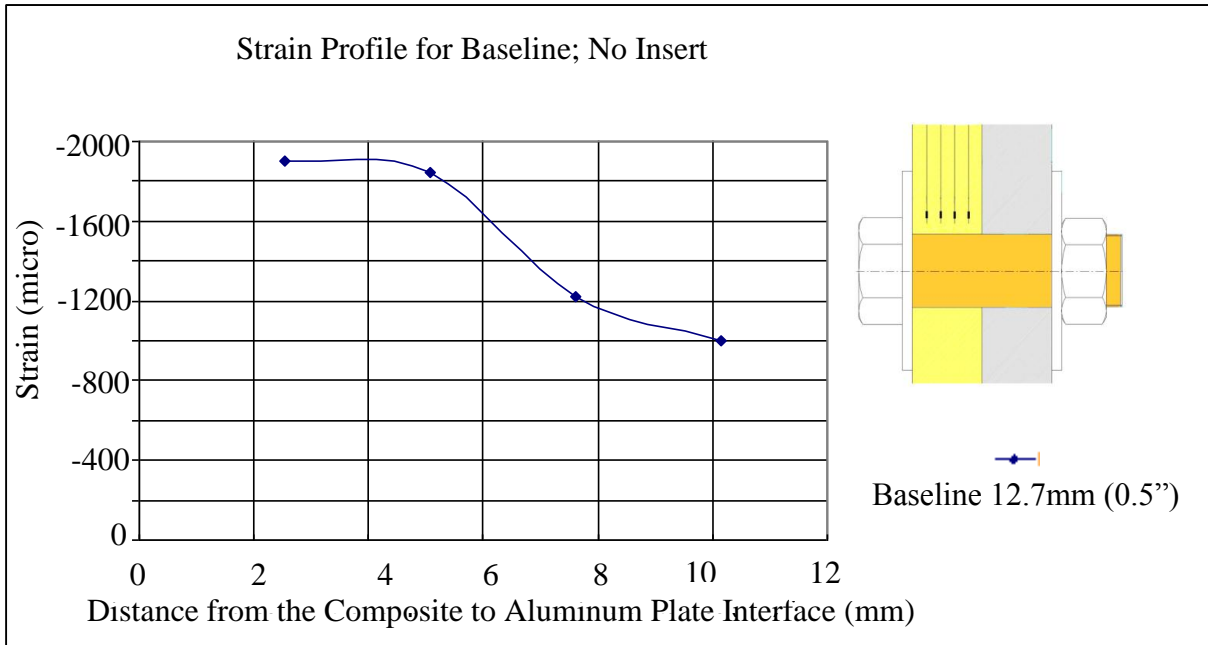


Figure 3-4: Baseline, 12.7mm (0.5") hole diameter with no insert

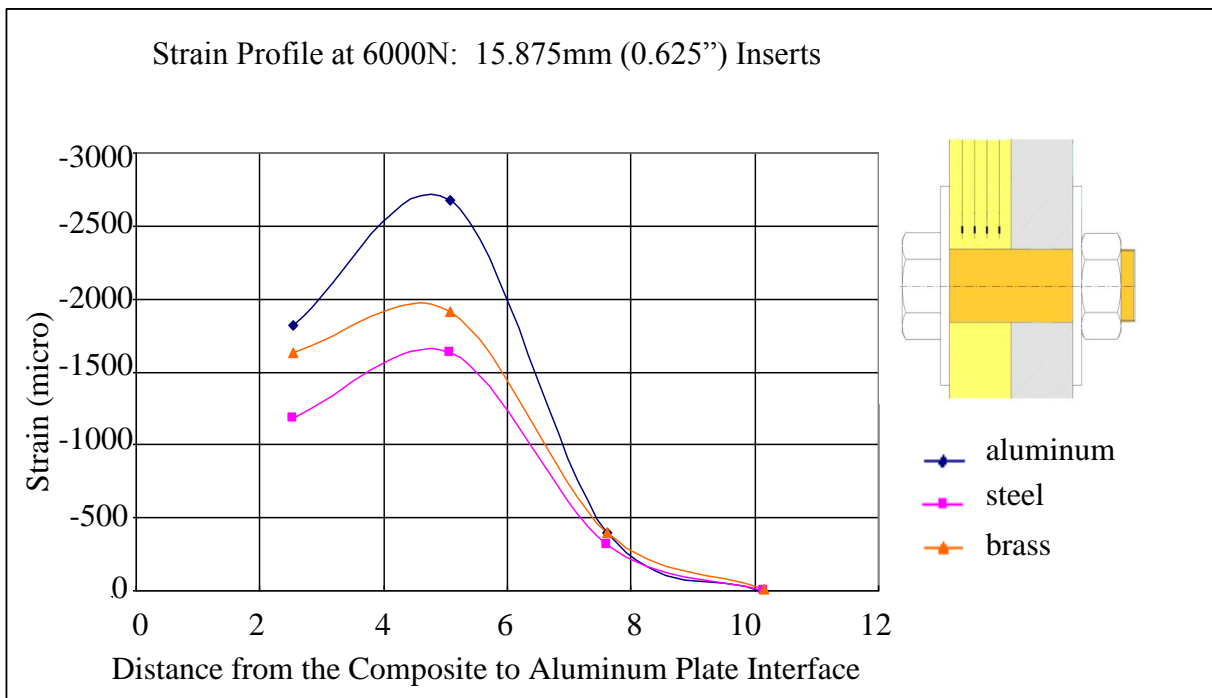


Figure 3-5: Strain profile of 15.875mm (0.625") insert for all three metals

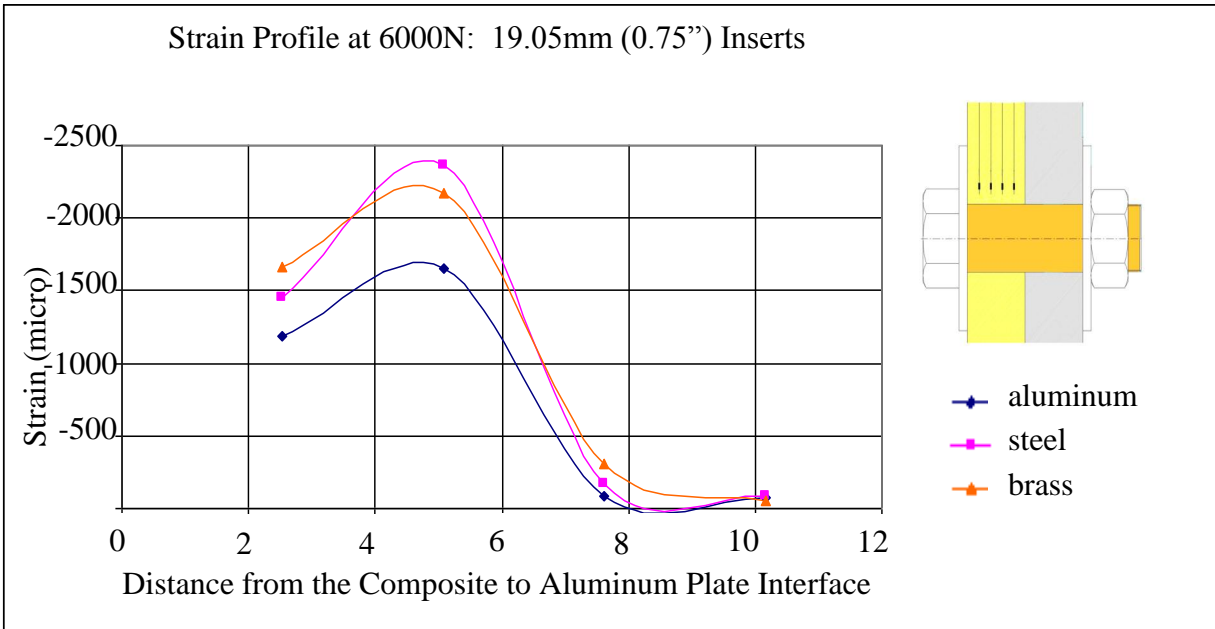


Figure 3-6: Strain profile of 19.05mm (0.75'') insert for all three metals

Configuration	N/mm
Baseline	9984
Al 0.625	9931
St 0.625	9991
Brass 0.625	9885
Al 0.75	9509
St 0.75	9588
Brass 0.75	8345

Table 3-2: Stiffness of the single-lap, bolted joint

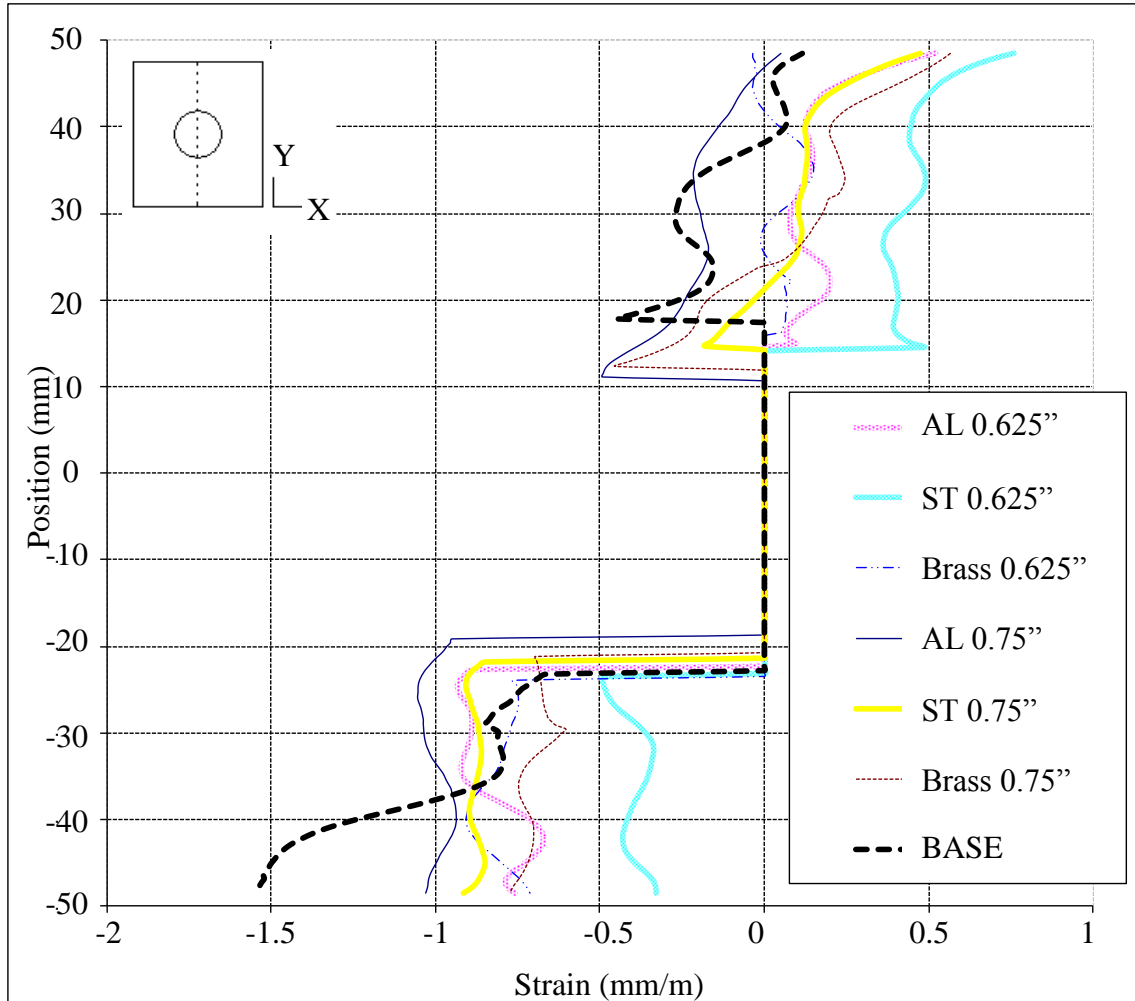


Figure 3-7: Surface strains in 1-direction taken down the center

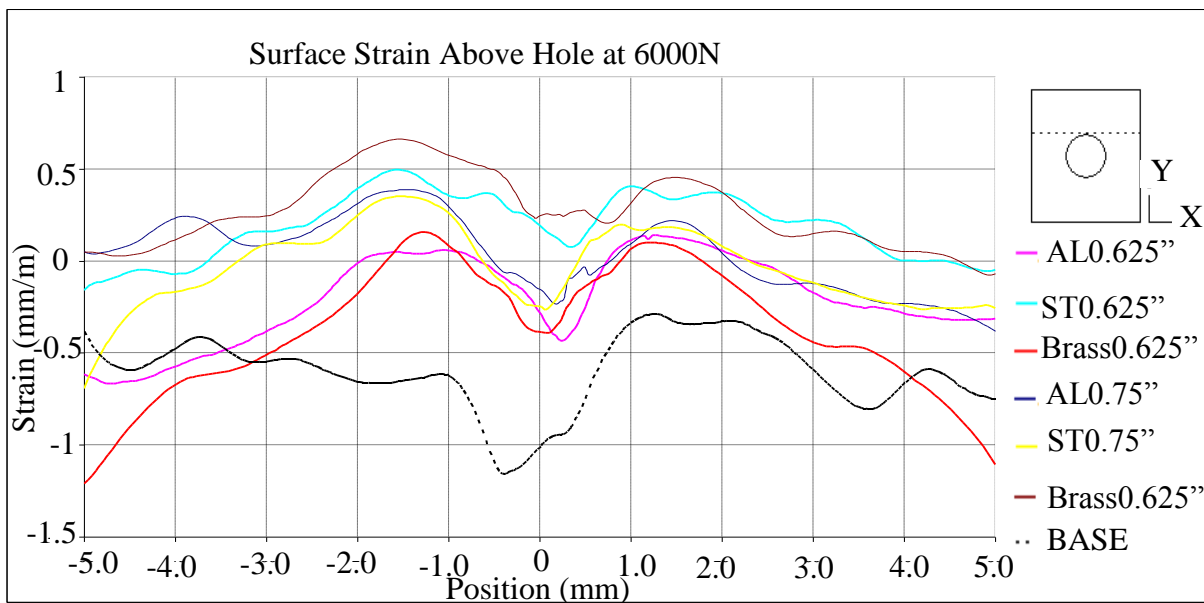


Figure 3-8: Surface strains in the 2-direction taken above the hole at 6000N

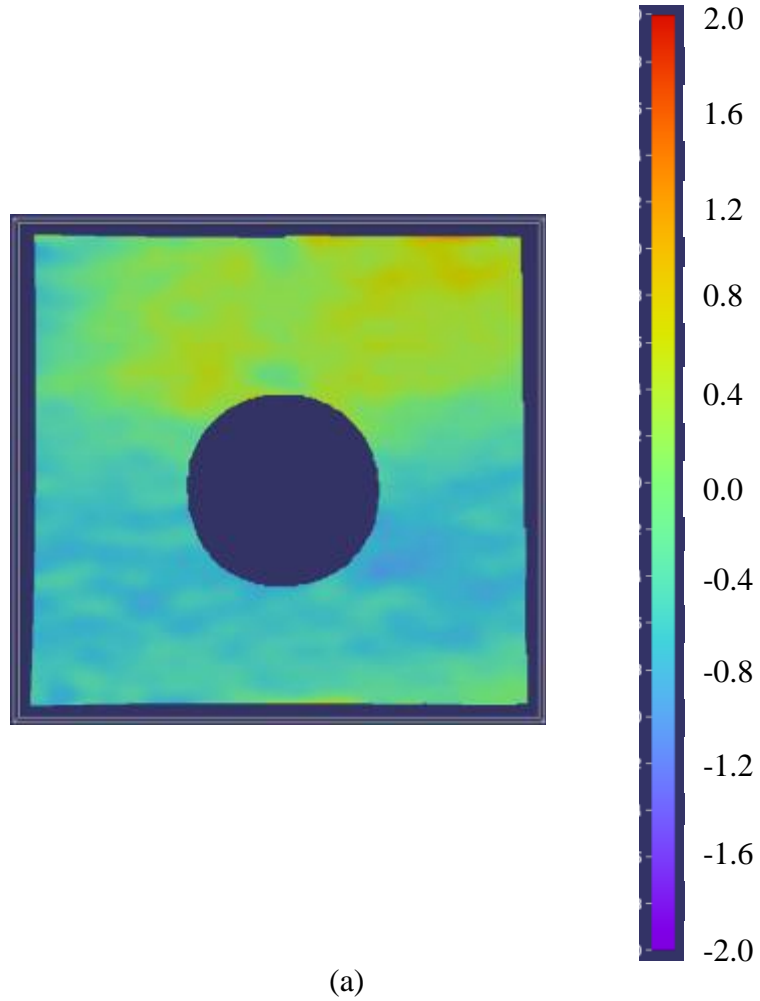
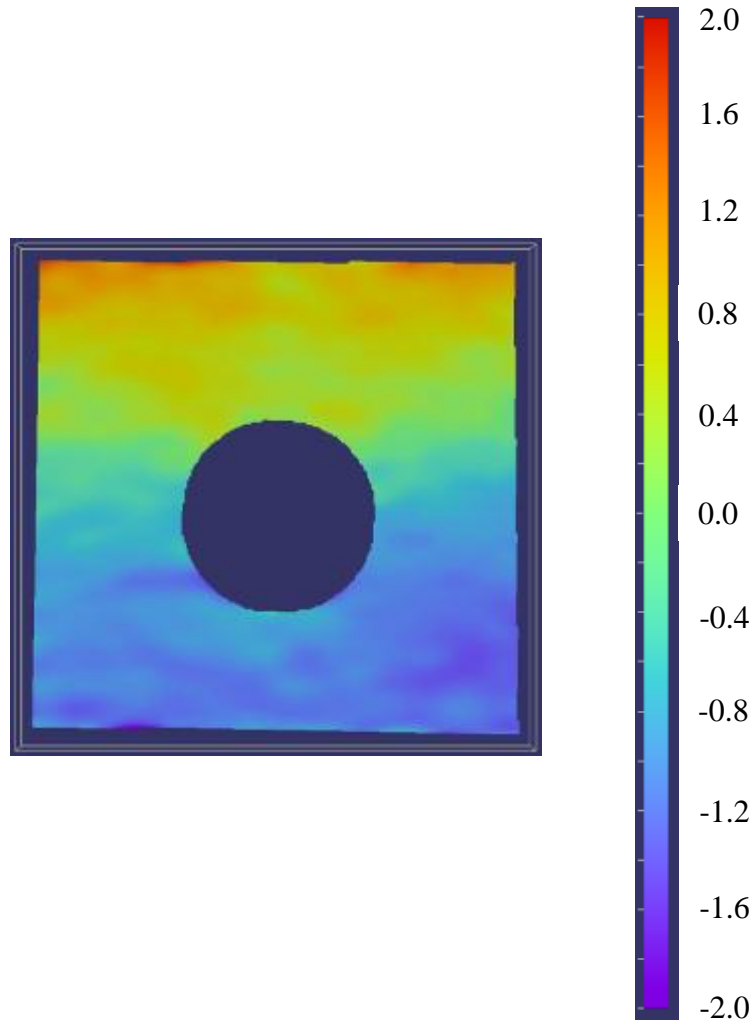


Figure 3-9: (a) 15.875mm (0.625") steel insert, (b) 19.05mm(0.75") aluminum insert

Figure 3-9 Continued



(b)

Steel 0.75 Insert				
Test	Location 1 DIC	Location 1 RSG	Location 2 DIC	Location 2 RSG
1	402	250	66	216
2	92	263	-39	224
3	314	258	68	225
Average	269	257	32	222

Table 3-3: Sensitivity test measurements; RSG to DIC comparison

## REFERENCES

## REFERENCES

- [1] Chutima, Surachate, Blackie, Alvin P. (1996). "Effect of pitch distance, row spacing, end distance and bolt diameter on multi-fastened composite joints" Composites Part A **27A**: 105-110
- [2] Pratt, John D., Pardoen, Gerard. (2002). "Influence of Head Geometry on bolted Joint Behavior" Journal of Aerospace Engineering **15**:4:136-153
- [3] Iancu, F. Ding, X. et al (2005) "Three-dimensional investigation of thick single-lap bolted joints." Experimental Mechanics **45**: 351-358
- [4] Nassar, Sayed A., Virupaksha, Vinayshankar L., et al. (2007). "Effect of Bolt Tightness on the Behavior of Composite Joints." Journal of Pressure Vessel Technology **129-1**: 43-51
- [5] McCarthy, M.A., McCarthy, C.T. (2004). "Three-dimensional finite element analysis of single-bolt, single-lap composite bolted joints: part II-effects of bolt-hole clearance" Composite Structures **71**: 159-175
- [6] McCarthy, M.A., Lawlor, V.P., et al. (2002) "Bolt-hole clearance effects and strength criteria in single-bolt, single-lap, composite bolted joints." Composites Science and Technology **62**: 1415-1431.
- [7] Chen, Wen-Hwa, Lee, Shyh-Shiaw, et al. (1995) "Three-dimensional contact stress analysis of a composite laminate with bolted joint." Composite Structures **30**: 287-297
- [8] McCarthy, M.A., McCarthy, C.T. (2003). "Finite Element Analysis of the Effects of Clearance on Single-Shear, Composite Bolted Joints." Journal of Plastics, Rubber and Composites **32**: 65-70
- [9] Herrera-Franco, Pedro, Cloud, Gary L., (1992). "Strain-Relief inserts for Composite Fasteners – An Experimental Study." Journal of Composite Materials **26**: 751
- [10] Camanho, P.P, Tavares, C.M.L., et al. (2005). "Increasing the efficiency of composite single-shear lap joints using bonded inserts." Composites: Part B **36**: 372-383.
- [11] Baldwin, C., Mendex, Alexis. (2005) "Introduction to Fiber Optic sensing with Emphasis on Bragg Grating Sensor Technologies; short course 102" Course Presented: SEM Annual Conference and Exposition on Experimental and Applied Mechanics
- [12] Lopez-Anido, R., Fifield, S. (2003). "Experimental Methodology for Embedding Fiber Optic Strain Sensors in Fiber Reinforced Composites Fabricated by the VARTM/SCRIMP Process". Structural Health Monitoring: 247 – 254.

[13] Isaicu, Gabriel (2006). “Three-Dimensional Strain Analysis of Single-Lap Bolted Joints in Thick Composites using Fiber-Optic Strain gages and Finite Element Method” Master’s Thesis, Department of Mechanical Engineering, MSU

[14] Marannano, G., Restivo, G. et al (2010). “GIUNZIONI BULLONATE FRA COMPOSITO E ALLUMINIO: STUDIO DEL GIOCO MEDIANTE FIBRE OTTICHE INGLOBATE NELLO SPESSORE”. AIAS – Italian Association for stress Analysis National Conference 2010.

## Chapter 4. Summary and Conclusions

### 4.1 Clearance Conclusions

Results from the clearance studies came in the form of both stiffness measurements, and through embedded fiber optic strain gages. Stiffness measurements found results similar to what was seen in thinner composite panel single-lap, bolted joints. The initial onset of clearance caused a dramatic drop in stiffness measuring about 11 percent. Stiffness remained at about the same value as clearance increased, until the maximum decrease in stiffness was seen at five percent. Strain readings from the fiber optic strain gages showed that most of the load is transferred through the area of the panel which is closest to the aluminum plate. Gage locations one and two read significantly higher than three and four, with gage location two reading the highest, indicating the area of the strain concentration. Initial clearance showed an increase in the strain concentration at gage location two. At three percent clearance strain was increased at all gage locations, with gage two still the highest. Further increase in clearance to five percent showed a leveling of the strain profile, but very high strain values through the thickness of the panel.

### 4.2 Insert Conclusions

The strength of the joint was determined through several means for the insert study. Stiffness calculations, embedded fiber optic strain gages, and DIC were employed. Using all three sources of measurement, a well rounded internal and external investigation was performed.

Stiffness measurements were interesting in that some explanation was necessary in order to initially understand them. The no-insert condition was actually the stiffest at 9.984 KN / mm. Applying the thinner diameter inserts of 0.625” outer diameter provided about the same stiffness as the baseline condition. Lastly the largest diameter inserts of 0.75” outer diameter provided the least stiff condition. The reason for this is that the cross sectional area of the composite plate on either side of the hole was reduced as the hole was made larger to accommodate the insert. Reducing the cross sectional area meant a higher strain in those regions, and a larger displacement, thus a lower stiffness. So in these experiments, stiffness did not predict the load carrying capability of the joint.

The fiber optic strain gages discovered trends in the strain profile through the thickness of the specimen above the hole, and a strain concentration. The concentration was once again at the location of gage two, as seen in clearance tests. For the inserts of the outer diameter of 0.625”, the steel material worked best. A strain value of 1634 micrometers was seen for the steel insert, as compared to 1911 micrometers and 2671 micrometers for the brass and aluminum inserts respectively. In the case of the larger diameter inserts, the aluminum insert performed best. Values of 1657 micrometers, 2175 micrometers, and 2362 micrometers for the aluminum, brass, and steel inserts respectively. What should be noticed, is that the insert with the highest modulus of elasticity performed best at the lower insert size, and the lowest modulus the poorest performing. However, for the larger diameter that trend reversed. The reason for this is the fact that as the stiffness decreased for the larger diameter inserts, the softer material was able to elastically deform to fill the hole and provide the best load distribution. It should be noted that the strain values between the smaller diameter inserts and that of the larger diameter inserts

should not be directly compared. As the hole widened to accommodate the larger inserts, the contact region moved closer to the gage locations, since the gages remained stationary in their position within the panel. Direct comparison of strain values can only be done between inserts of similar size.

Lastly, surface strain measurements were compiled using a 2-D digital image correlation system. The best performing insert was determined by locating the condition that minimized the strain value seen above the hole, where contact is made between the bolt and the hole. Measurements found the same results the fiber optic strain gages found, that being the steel was the best insert for the smaller insert size, and the aluminum the best insert for the larger size, and overall any insert performed better than the no insert condition. DIC images showed that there is compression below the hole due to bending, and tension in the rest. There is an exception of a small area of compression is seen just above the hole due to the contact of the bolt.

#### 4.3 Design Recommendations

In order to successfully implement the composite plate into field use, design recommendations regarding the studied fastening parameters must be determined. The previous studies have used internal and external methods of measuring the effects of clearance and inserts on the joint strength. Overall, it was determined that clearance has a negative effect on joint strength. Any fastening design should try to make the bolt to hole connection a snug fit, of approximately zero percent. If clearance reaches a value of three percent, the panel should be removed from service. Inserts were found to help the performance of a joint significantly. An aluminum insert of 0.75” outer diameter should be used.